Christoph Bichler, BSc

Automated Detection of Security-Relevant Objects in Airport Surface Movement Radar

Master's Thesis

Graz University of Technology

Institute of Electrical Measurement and Measurement Signal Processing
Head: Univ.-Prof. Dipl-Ing. Dr.techn. Georg Brasseur

Supervisor: Ao.Univ.-Prof. Dipl.-Ing. Dr.techn. Axel Pinz

Graz, January 2015

Statutory Declaration

I declare that I have authored this thesis independently, that I have not used other than the declared sources/resources, and that I have explicitly marked all material which has been quoted either literally or by content from the used sources.

Graz, ______________________ ______________________

Date Signature

Eidesstattliche Erklärung[1]

Ich erkläre an Eides statt, dass ich die vorliegende Arbeit selbstständig verfasst, andere als die angegebenen Quellen/Hilfsmittel nicht benutzt, und die den benutzten Quellen wörtlich und inhaltlich entnommenen Stellen als solche kenntlich gemacht habe.

Graz, am ______________________ ______________________

Datum Unterschrift

[1]Beschluss der Curricula-Kommission für Bachelor-, Master- und Diplomstudien vom 10.11.2008; Genehmigung des Senates am 1.12.2008

Abstract

The goal of this thesis was the design, implementation and evaluation of a methodology for automated detection of security-relevant objects in radar video produced by *Surface Movement Radars* (SMR) used for air traffic control. During bad visibility situations, such as dense fog or heavy rain, these radars are the only way of monitoring positions and movements of non-cooperative objects on the ground that might pose a threat for other ground traffic.

Due to commercial interest, little information about existing approaches for SMR target detection is publicly available. Therefore, methods from general radar signal processing and image processing were evaluated regarding their applicability to the problem at hand. This was done based on a data analysis performed on available operational SMR data. The resulting modular design for an SMR target detection scheme consists of a number of steps. First, a preprocessing step on radar signal level incorporating *Constant False Alarm Rate (CFAR)* processing is performed. This is followed by a *Target Candidate Formation* step, applying methodologies from image processing, such as *Region Growing*, *MSER* and *Maxima Detection*. Resulting candidates are then classified in a *Target Candidate Classification* step based on spatial and temporal properties, incorporating *Interacting Mixed Model (IMM) Kalman Filters* and heuristics defined in the data analysis.

The presented target detection scheme was implemented and integrated into an existing surveillance system and installed at Bucharest Otopeni Airport. To measure the performance of the detection scheme, a number of evaluation methods including *User Experience Tests*, *Probability of Detection* analysis and *Long Term Evaluation* were performed. The evaluations showed satisfactory results and indicated that operational use of the presented scheme is possible, given that manual adjustments are performed on a regular basis.

Kurzfassung

Ziel dieser Diplomarbeit waren Design, Implementierung und Evaluierung einer Methode zur Erkennung Sicherheits-relevanter Objekte in Surface Movement Radar (SMR) Video. Diese speziellen Radarsysteme kommen bei der Überwachung von Bodenbewegungen auf Flughäfen im Zuge der Flugsicherung zum Einsatz. Herrscht schlechte Sicht, so bilden diese Systeme die einzige Möglichkeit um nicht-kooperative, möglicherweise den Bodenverkehr gefährdende, Objekte überwachen zu können.

Da es sich hierbei üblicherweise um geschlossene Systeme handelt, ist wenig Information zu bestehenden Detektionsmethodologien frei verfügbar. Aus diesem Grund wurden generelle Methoden aus Radar-Signalverarbeitung und Bildverarbeitung bezüglich ihrer Anwendbarkeit auf das Problem untersucht. Dazu wurde zuerst eine Datenanalyse auf operationalen Datensätzen durchgeführt. Basierend auf den Resultaten wurde eine modulare Detektionspipeline entworfen.In einem Vorverarbeitungsschritt auf Radarsignalebene kommen *Constant False Alarm Rate (CFAR)* Methoden zum Einsatz. Im *Target Candidate Formation* Schritt werden Target-Kandidaten aus dem Radarbild extrahiert. Dabei kommen Methoden aus dem Bereich der Bildverarbeitung wie *Region Growing*, *MSER* und *Maxima Detection* zum Einsatz. Resultierende Kandidaten werden im *Target Candidate Classification* Schritt unter Anwendung von *Interactive Mixed Model (IMM) Kalman Filtern* und aus der Datenanalyse definierten Heuristiken klassifiziert. Die präsentierte Methode wurde in ein bestehendes Bodenverkehrs-Überwachungssystem integriert und am Bukarest Otopeni Flughafen installiert. Eine Reihe von Evaluierungsmethoden kamen zur Überprüfung der Ergebnisse der präsentierten Methode zum Einsatz: *User Experience Tests*, *Probability of Detection* Analysen und *Long Term Evaluation*. Die Evaluierungen zeigten zufriedenstellende Leistungen, sodass ein operationaler Einsatz unter Einhaltung von regelmässigen manuellen Anpassungen durchaus möglich ist.

Acknowledgements

This thesis marks the end of a wonderful time I was privileged to spend at Graz University of Technology. First of all I would like to thank my parents deeply for their enduring support and for encouraging me to go to university. Without you, this would not have been possible! Many thanks also go to my sister Sarah, for offering encouragement in tough times and for being the funniest person around. During my time at Graz University of Technology I met a lot of great people who made this chapter of my life story the most memorable so far. Thank you for all the successful cooperations and the fun we had. Also, thanks to my friends and (former) roommates for the tons of fun during these years!

I would like to thank AviBit GmbH for the opportunity to work in the interesting field of air traffic control and for their support during the time of this thesis. The Austrian Research Promotion Agency (FFG) supported me and this thesis very much by granting an "Innovationsscheck", which supports cooperation between university and industry and funds works like diploma theses. I would furthermore like to thank my supervisor Professor Axel Pinz for his guidance during the time of this thesis and for always being helpful and understanding. Thank you! I would also like to thank Karl Voit, who created the LaTeX template used for writing this thesis.

Last but not least, I would like to thank my girlfriend Peggy for always being there for me and for being the great person you are! Thank you for also being so understanding about not spending as much time with each other during the phase of completing this work.

Contents

Abstract iii

1. Introduction 1

2. State of the Art SMR Target Detection for Airport Surveillance 5
- 2.1. Data Analysis . . . 6
  - 2.1.1. Intensity . . . 8
  - 2.1.2. Location . . . 8
  - 2.1.3. Movement / Trajectory . . . 9
  - 2.1.4. Spatial properties . . . 9
  - 2.1.5. Contrast . . . 10
- 2.2. Constant False Alarm Rate (CFAR) Detection . . . 10
  - 2.2.1. Range CFAR Detection . . . 10
    - 2.2.1.1. Cell-Averaging CFAR (CA-CFAR) . . . 14
    - 2.2.1.2. Order-Statistics CFAR (OS-CFAR) . . . 17
    - 2.2.1.3. Variability Index CFAR (VI-CFAR) . . . 19
  - 2.2.2. Temporal (Clutter Map) CFAR Detection . . . 23
  - 2.2.3. Hybrid CFAR Detection . . . 26
- 2.3. Tracking for Target Detection . . . 27
- 2.4. Summary . . . 29

3. Design and Implementation of a Target Detection Scheme for SMR Data 31
- 3.1. Radar Data Preprocessing . . . 33
  - 3.1.1. Data Normalization . . . 33
  - 3.1.2. CFAR Processing . . . 35
- 3.2. Target Candidate Formation . . . 37
- 3.3. Target Candidate Classification . . . 39
  - 3.3.1. Spatial Classification . . . 40

3.3.2. Temporal Classification 43
3.4. Implementation Details 52

4. Experimental Evaluation on Real-World Datasets 54
4.1. Performance for Critical Traffic Situations 55
4.2. Performance Analysis For Small Targets 60
4.3. User-Experience Test, Long-Term Evaluation 65

5. Conclusion and Future Work 69

A. Surface Movement Radars (SMR) for Airport Ground Control 75
A.1. Image Acquisition and Functionality 75
A.2. Clutter and Noise in SMR Images 78

B. Reference Radar Setup at Bucharest Airport 82

Bibliography 87

List of Figures

2.1. General architecture of range CFAR detectors 12
2.2. CA-CFAR performance on a 1D signal in different signal situations 16
2.3. OS-CFAR performance on a 1D signal in different signal situations 18
2.4. Complex Spatial/Temporal CFAR scheme 27

3.1. Processing pipeline from raw radar data to extracted targets for proposed automated target detection 32
3.2. Flow chart of Target Detection Scheme Part 1 - Data Normalization and CFAR Processing 34
3.3. Comparison between raw and CFAR-filtered SMR images . . 36
3.4. Flow chart of Target Detection Scheme Part 2 - Target Candidate Formation 39
3.5. Flow chart of Target Detection Scheme Part 3 - Target Classification 41
3.6. Mapping of targets across radar scans: Track candidate after first scan 45
3.7. Kalman track candidate 47
3.8. Track Initiation after a number of consecutive object detections 49
3.9. Kalman Track, Predict/Update Cycle 51

4.1. Sample radar data sequence of a landing aircraft 57
4.2. False targets on Runway South during analysis of landing aircraft 58
4.3. Radar returns at Runway North during evaluation of detection scheme performance for starting aircraft 59
4.4. Visualized route of the performance evaluation and coverage test at Bucharest Airport 61

4.5. Visualization of probability of detection analysis results (Both Radars, Tracked) 67

A.1. A sample SMR installation 76
A.2. Visualization of tangentially growing samples with radial distance of the radar sensor 77
A.3. The radar shadowing effect 78
A.4. A sample SMR image of Hamburg Airport (good weather) . . 79
A.5. A sample SMR image of Hamburg airport (rain) 80

B.1. Map of the Bucharest Otopeni Airport (SMR locations marked) 84
B.2. Visualization of areas without radar coverage for SMR-West at Bucharest Airport 85
B.3. Visualization of areas without radar coverage for SMR-East at Bucharest Airport 86

List of Tables

2.1. Computation of an adaptive threshold based on *VI* and *MR* of reference cell window halves A and B and the corresponding methods (adapted from [23]) 21

4.1. Results of detection analysis for landing aircraft (Runway South) 56
4.2. Results of detection analysis for starting aircraft (Runway North) 59
4.3. Results of probability of detection analysis for test drive without incorporating temporal progression of target 62
4.4. Results of probability of detection analysis for test drive, taking temporal progression of target into account 64

B.1. Radar sample sizes in radial distance of the radar for reference setup at Bucharest Airport 83

1. Introduction

An efficient handling of aircraft ground movements is becoming increasingly important as the numbers of flights handled at airports constantly keep growing, while infrastructure remains the same. In addition, ground movement safety is becoming more important, as the rising number of flights should under no circumstances compromise the safety of airport ground movements.

Air traffic control providers use so-called *Advanced Surface Movement Guidance and Control Systems* (A-SMGCS) to safely and efficiently guide aircraft during ground movements at airports. These surveillance systems help the controllers keep an overview of the situation on the airport movement areas and highly increase the number of safe movements which can be performed simultaneously. A-SMGCS systems typically receive inputs from a number of surveillance sensors of cooperative nature (where all surveilled objects identify themselves using some sort of transponder). These systems typically utilize specialized *Surface Movement Radars* (SMR) to have a means of non-cooperative surveillance. The air traffic controllers are provided with a visualization of the echoes of these radars by the A-SMGCS system for the purpose of situation awareness.

The "radar images" produced by these radars typically suffer from a number of shortcomings. Due to the large area a radar has to cover at an airport, the resolution for a single radar cell is rather low (typically three to ten meters). This leads to the fact that radar images are rather low in detail. Due to this low level of detail, it is often hard for the human eye to recognize which objects produced a certain radar echo.

Because of the nature of a radar sensor, any reflective object will produce echoes in a radar image. On the movement areas of an airport the number of reflective objects is vast, which leads to a lot of visual clutter in SMR imaging as not all of these objects are security relevant. Furthermore, depending on the specific radar in use, rain or snow (but also fog) can highly increase the noise levels in radar echoes. This makes a visual distinction between important, security-relevant radar returns and clutter and noise returns even harder. As during these weather situations the possibility for visual inspection of the ground from the tower becomes seriously impaired, the air traffic controllers have to rely on the output of the A-SMGCS system.

To aid the air traffic controllers with the distinction between clutter and security-relevant radar echoes as well as to prevent human error, an automated detection of security-relevant objects in radar images is needed. Automated target detection also opens doors for automated alarm generation based on predicted object movements of observed trajectories. The main requirements for automated target detection in this context are robustness of detection, low number of false targets and low computational load due to real-time requirements of the system.

As this very specialized application of radar technology is of commercial interest, publicly available literature and related work is mostly limited to general radar signal processing techniques. This master's thesis presents a methodology for the automatic detection of security-relevant objects in SMR images which is based on adaptive filtering of the radar data, formation of target candidates contingent on image processing methods and classification of the target candidates based on spatial and temporal properties.

The structure of this thesis is as follows.

Chapter 2 contains the results of a data analysis, which was performed to extract a number of properties on which the ”targetness” of SMR radar echoes can be defined. It further gives an overview of methods from literature used within the proposed target detection scheme.

In Chapter 3 the conceptual design of the proposed target detection scheme and its implementation is presented.

The conception of evaluation methodologies for the target detection scheme, the results from operational data and their discussion can be found in Chapter 4.

A conclusion about the outcome of this work and possible future work are presented in Chapter 5.

In Section A of the appendix, an introduction to radar as an imaging sensor is given for unfamiliar readers. The reference radar setup at Bucharest Otopeni Airport which provided operational data for this work is described in Section B of the appendix and concludes the thesis.

2. State of the Art SMR Target Detection for Airport Surveillance

The goal of this thesis was to design and implement a robust way for detecting security-relevant targets in SMR data for airport surveillance. After starting literature research to determine the current state-of-the-art in the field, it soon became clear that this rather specific and practical problem is not targeted much in current research. Furthermore, it is impossible to determine which methodology for target detection is used in commercial state-of-the-art SMR surveillance systems, as this is vital know-how of the selling companies. Due to this lack of publicly available related work, it is difficult to relate to or extend existing methodologies for SMR target detection. Therefore, it was decided to investigate on how the design of a target detection scheme should be approached and if more general methods for target detection from radar processing and image processing may be applicable to this problem.

To get a better understanding about the nature of the data, a data analysis was conducted at first. The goal of this data analysis was to find properties, based on which a target detection for airport surveillance could be performed. This data analysis and the elicited properties are described in Section 2.1.

Methods for the removal of unwanted radar echoes or so-called "clutter" are described in general radar signal processing literature. These general target detection methods are adaptive filtering methods called *Constant False Alarm Rate* (CFAR) detectors. Due to the highly differing requirements and restrictions in radar applications, such general methods need to be evaluated for their applicability to a certain application first. The methods and the evaluation with respect to applicability to airport radar surveillance are presented in Section 2.2.

A number of weaknesses of radar as a surveillance sensor can be overcome by tracking detected radar targets. Missed target detections due to short loss of physical radar coverage can be extrapolated from the trajectory of the tracked object. A number of commonly used methodologies for tracking of radar targets are described in Section 2.3.

2.1. Data Analysis

For a better understanding of how to differentiate between relevant radar returns (target echoes) and non-relevant radar returns for safe ground movements (non-target echoes) in SMR data, a data analysis was conducted. The analysis was done on a number of characteristic sequences of radar data recorded at Bukarest Otopeni Airport. The setup at this airport was the main source of radar data and will hence be referred to throughout this work. It is described in detail in Section B of the Appendix.

The characteristic sequences were recorded during regular daytime airport operation and during different weather situations. This ensures realistic data with all different types of security-relevant objects that will typically be encountered on movement areas in airport environments. Objects in airport environments differ greatly in various ways, such as their size, shape and movement velocity just to name a few. The resulting radar echoes of these objects and their trajectories should hence also differ greatly. The goal of the data analysis was to find a way to distinguish between radar echoes produced by security-relevant objects and those produced by other, non-security-relevant objects. For this classification, a number of properties were to be elicited which could be used for the classification of radar echoes into target and non-target echoes. The resulting properties were then used to design a target detection scheme for robust target detection.

During the analysis, it quickly showed that a robust detection of targets contingent on the shape of the radar echo was not possible. Reasons for this were the very low spatial resolution of the radar (see Section B for the sample sizes at the reference site) as well as the fact that the shape of the echoes may change rapidly from one radar scan to the next. These changes in appearance can be explained when looking closer at the nature of how image acquisition for SMRs works. For the shape of the echo, the angular position of the target to the radar plays a very important role. Depending on the object's shape and orientation, the energy sent by the radar may be reflected back to the radar (and registered) or away from the radar (and hence may not result in a strong intensity echo). Furthermore, objects within the line-of-sight between the radar and an object of interest may also reflect parts of the sent radar energy away before it could reach the actual object. This would hence decrease the intensity of the echo for the target of interest, even though it may itself be highly reflective. The observation that the radar echoes produced by the same object can and will look completely different in consecutive radar scans, leads to the conclusion that object recognition and tracking based on the shape of radar echoes will not work well for this application. The unfamiliar reader may refer to Section A.1 of the Appendix, where the image acquisition process for SMR is described in coarse detail.

After analyzing a number of evaluation sequences, it can be summarized that the "targetness" of radar echoes in SMR images in airport environments is dependent on a number of properties:

- The *intensity* of a radar echo
- The *location* of a radar echo
- The *movement* or *trajectory* of a radar echo
- The *spatial properties* of the radar echoes (area of connected radar echoes of similar intensity, ratio of width/length of these areas)
- The *contrast* of intensity to neighboring radar echoes (visual difference)

The importance of these properties for target detection is motivated shortly in the following subsections.

2.1.1. Intensity

The intensity of a radar echo is a measure of how reflective the surface of an object is. As we expect most of the security-relevant objects on an airport to be metallic (aircraft, cars, other ground vehicles and equipment), high intensity of the radar echoes are a pointer to classify these echoes as targets. However, buildings, concrete curbs, snow, trees, wet grass and rain also result in very high radar intensities. This is the main reason why classification based on radar echo intensity alone does not work and why other properties of ”targetness” need to be incorporated in target detection.

2.1.2. Location

Most security-relevant objects for safe ground operation at airports are encountered in areas where aircraft movements are performed. Such areas are called movement areas and contain runways, taxiways, aprons and terminal parking areas of the airport. In these areas, objects might form an obstacle or cause a threat of colliding with moving aircraft and need to be detected to prevent dangerous situations. A plausible situation is an airport maintenance car driving on a runway, where an aircraft is scheduled to land shortly. Clearly, the radar echo of the car on the runway needs to be classified as security-relevant in order to automatically detect such dangerous situations and prevent accidents.

On the other hand, non-movement areas are less probable to contain security-relevant objects. The areas between and along the taxi- and runways belong to these non-movement areas. If radar echoes with high intensity are encountered in these areas, with high probability they are produced by fixed non-security-relevant objects. Examples are antennas, other fixed metallic objects or buildings, which produce radar echoes with high intensity but do not pose a threat to safe airport ground movements.

The probability of radar echoes being security relevant is hence affected by their location at the airport and is important for classification.

2.1.3. Movement / Trajectory

As described in the previous subsection, high intensity radar echoes in non-movement areas are, with high probability, produced by fixed non-security-relevant objects. However, if intended or by accident, any moving vehicles might still enter non-movement areas and possibly cause a security threat. In this case it helps to have information about the trajectory of a radar echo to classify radar echoes in non-movement areas. In these areas, moving objects with high radar intensities are highly likely to be security-relevant,

while objects which do not move but also produce high radar echo intensities are likely to not be security relevant.

More generally, on movement areas information about the trajectories of radar echoes is important. Based on the trajectories of objects, a prediction of future movement could be made and dangerous situations could potentially be detected early and mitigated. Moreover, in some cases it might be of interest to classify static objects within movement areas as non-security-relevant (for example, parked aircraft on apron areas).

2.1.4. Spatial properties

As stated at the beginning of this section, unfortunately the data analysis showed that the resolution of radar cells is too low to be able to detect security-relevant objects based on their shape. However, spatial properties, such as the area of adjacent radar cells with similar intensities or the length-width ratio of these areas can still be helpful to distinguish between target and non-target radar echoes. The length-width ratio, for instance, can be used to identify radar echoes produced by concrete curbs (The evaluation sequences showed that curbs produce very elongated connected radar echoes).

2.1.5. Contrast

In aforementioned situations of rain- or snowfall the overall radar echo intensity levels rise due to the reflectivity of raindrops and snowflakes. In this case, the intensity levels alone do not yield reliable information anymore if a cell is part of a target or not.However, the contrast to radar echoes of neighboring radar cells can give information as to wheter a tested radar echo should be considered to be part of a target or not. A high contrast (higher intensity than in neighboring radar cells) means that a cell ”stands out”, which points to the fact that the cell may be part of a target. This is also valid for a number of cells with similar intensities connected to each other which stand out from their surroundings. If the intensity of a cell however is very uniform with neighboring radar cells (the contrast is low) over an area larger than the largest expected target, the cell is probably not part of a target.

2.2. Constant False Alarm Rate (CFAR) Detection

In this section, the so called *Constant False Alarm Rate* detection for radar clutter removal is presented. These methods from general radar signal processing can roughly be grouped into three categories:

- **Range-based Approaches**, clutter removal based on spatial statistics (described in Section 2.2.1).
- **Temporal Approaches**, clutter removal based on temporal statistics (described in Section 2.2.2).
- **Hybrid Approaches**, a mixture of range- and temporal-based CFAR (described in Section 2.2.3).

2.2.1. Range CFAR Detection

The primary goal of SMR used for air traffic control is to detect all targets inside the surveillance area and to estimate their position, size, orientation and velocity. Unfortunately, the received energy at the radar receiver does not only consist of signal echoes (reflected energy of actual targets), but also of noise, energy reflected from clutter and possibly interfering energy from other radars.

As Rohling describes in [21], the task of separating targets from clutter and noise would be easy if the targets were observed in front of an empty or statistically completely known noise or clutter background. Should this be the case, then the decision of whether the radar echo of a currently-tested radar cell should be considered a target could be reached by simply testing if the echo amplitude for the cell exceeds a fixed threshold. This global threshold would only depend on the clutter or noise statistics and could easily be computed.

However, in practical radar applications these noise and clutter levels are completely unknown and will also vary in time, position and intensity. This complicates the separation of unwanted clutter from actual targets in the radar images and makes it a much more difficult task. Furthermore, different types of clutter with greatly varying spatial dimensions may be present.

Rohling agreeingly states in [21], that the clutter in real-world radar applications is a complex space and time variant stochastic process. He says that these conditions call for an adaptive procedure operating with a varying threshold, instead of a fixed one. He says that such a varying threshold should be determined in accordance to the locally observed clutter situation with different spatial extension, intensity and fluctuation in the background of the target echoes. According to Rohling, the first step of a radar target detection procedure should be to estimate the unknown parameter of a statistical model which describes the clutter background around the target echoes.

In the case of so-called range CFAR procedures, the unknown statistical parameters of background clutter are always estimated by analyzing the radar signal within a fixed window size, which is oriented in the range direction surrounding the current *cell-under-test* or CUT (the radar cell which is currently tested to be a target) [21]. From this data, an adaptive threshold is generated, based on the estimated parameters of background clutter. Figure 2.1 shows the general detection procedure for range CFAR procedures.

These procedures work with the objective of maximizing the target detection probability, while maintaining a very low and *Constant False Alarm Rate* (hence the name CFAR). The *False Alarm Rate* (also known as *False Positive Rate* in statistics) is the ratio:

$$FAR = \frac{N_f}{N_{rc}} \tag{2.1}$$

with N_f being the number of radar cells falsely classified to be a target and N_{rc} being the overall number of radar cells in the observation area. Usually a very small FAR is chosen and the CFAR procedure is designed accordingly to keep it constant.

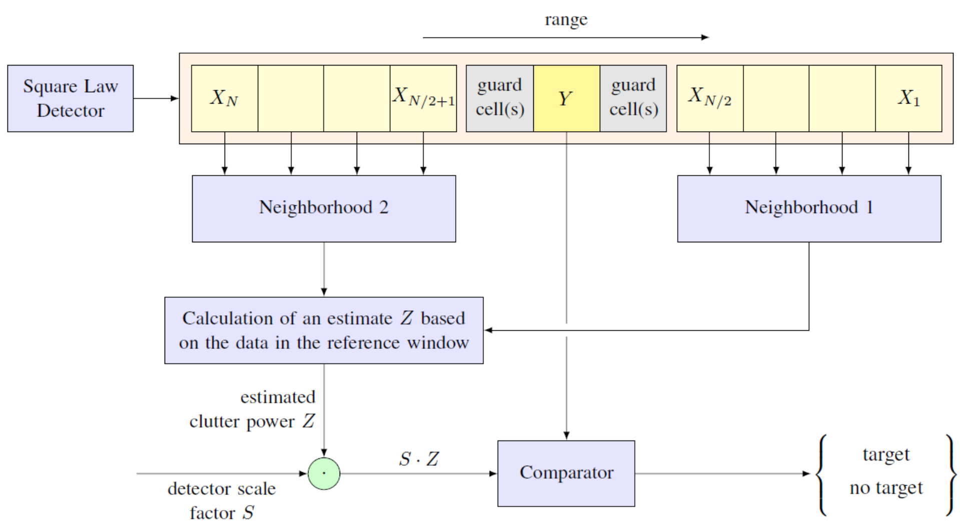

Figure 2.1.: General architecture of range CFAR detectors (taken from [22])

The system of reference cells, guard cells and cell-under-test in Figure 2.1 is referred to as *sliding-window* as it "slides" along the samples of a beam in range direction [21].

The cells $X_N ... X_{N/2+1}$ and $X_{N/2} ... X_1$ are called reference cells and are the cells which are being taken into account for estimating the background clutter parameters. The group of reference cells $X_{N/2} ... X_1$ is referred to as the *leading part*, while $X_N ... X_{N/2+1}$ is called the *lagging part* of the reference cells (with respect to the range direction away from the radar). Note that the X_i are vectors in azimuth direction for two dimensional signals, as in the case of SMR images.

The guard cells shown in Figure 2.1 are a number of cells directly adjacent to the current CUT, which will not play a part in the estimation of the clutter background parameters. They have been introduced to reduce the effect of "self-interference" [21]. Targets extending over more than one radar cell would interfere with the background estimate as they would be part of the reference cells.

Rohling states in [22] that the adaptive target detection threshold, denoted by T, may be computed as

$$T = S.Z \tag{2.2}$$

where S is a scaling factor for the background clutter estimate Z (as depicted in Figure 2.1) and can be computed as

$$S = ln \frac{1}{P_{fa}} \tag{2.3}$$

s with P_{fa} being the chosen probability of false alarm. Because of the logarithmic nature of the receiver (see Section A of the Appendix for details) in airport surveillance applications, S is often depicted as an additive rather than a multiplicative factor in other publications (for example in [7]).

As already stated, clutter in real radar applications can be caused by different physical sources and will therefore follow different probability distribution models (a few examples for types of clutter in airport environments are described in the Appendix, Section A).

Range-CFAR techniques will yield distorted background level estimates if the radar echoes of different clutter origin are present in the reference cells for a CUT (as the statistical requirement of identically distributed random clutter variables for estimation is not fulfilled [21]). Therefore, the fixed size of the sliding-window (and hence the number of reference cells) has to be chosen appropriately to the typical range extensions of homogeneous clutter areas beforehand. In the case of radar processing in airport environments, different types of clutter with greatly varying spatial extension are present, which makes this choice for the range extension of the sliding-window very troublesome. Furthermore, the spatial extension of the targets to be detected has to be known or estimated a priori, as the guard cell size has to be chosen.

Because of the different clutter types in airport environments and their different spatial extensions, the use of range-CFAR filters alone will yield poor estimates of the background clutter levels and make their use inpracticable.

Nevertheless, a number of range-CFAR methods will be presented in the following sections, as a combination with another form of CFAR filter can lead to better results (these combined methods are described in Section 2.2.3).

The different range-CFAR techniques differ in which statistical parameter of the background clutter is estimated and in the assumptions which are made about the background and target signal models. Target detection with CFAR techniques have generally been a well-researched area in radar signal processing for over four decades. The range-CFAR methods described in the following sections are just a small selection of the many known CFAR procedures in literature and were chosen due to the applicability to target detection in airport ground radar and the real-time constraint this implies.

2.2.1.1. Cell-Averaging CFAR (CA-CFAR)

The CA-CFAR processor for radar target detection was already introduced in 1968 by Finn and Johnson in [9]. In this simple approach, the average clutter amplitude level in all reference cells around the CUT is used to calculate a locally adaptive threshold. Therefore, the estimate Z for the background clutter as depicted in Figure 2.1 is the arithmetic mean of the radar signal echoes in all reference cells:

$$Z = \frac{1}{N} \sum_{i=1}^{N} X_i \tag{2.4}$$

This method is based on the assumption that a target is present in Gaussian distributed clutter. It has been shown that this method is optimal for homogeneous Gaussian clutter situations if the number of reference cells is large enough (as claimed by Zhao in [28]). However, the estimation of the clutter background level will be bad at "clutter edges", where different types of clutter are present in the reference cells (the clutter is inhomogeneous), as the method implicitly assumes homogeneous clutter background.

Furthermore, this method assumes single-target situations. In case of a multiple target situation, where another target is present in the reference cells, an actual target may be suppressed (these observations were described in [20]). Rohling gave a summary of the CA-CFAR procedure in [22] and visualized its performance in four different signal situations, which can be seen in Figure 2.2.

As it is clearly visible in plot (d), one target is not detected, because the detection threshold is raised by another spurious target within the reference area.

Multiple target situations will often arise in airport ground radar (for example, fuel trucks, mobile staircases or luggage carts approaching an aircraft), which makes this method alone impracticable.

Variations to improve the method have been proposed, which calculate seperate means for the "leading" and "lagging" part of the sliding window (refering to the two blocks of reference cells in Figure 2.1): the so-called *Cell-Averaging Greatest-Of CFAR* (CAGO-CFAR) [11] and the *Cell-Averaging Smallest-Of CFAR* (CASO-CFAR) [25].

These variations simply select the bigger respectively smaller of the computed means to compute the threshold for target detection.

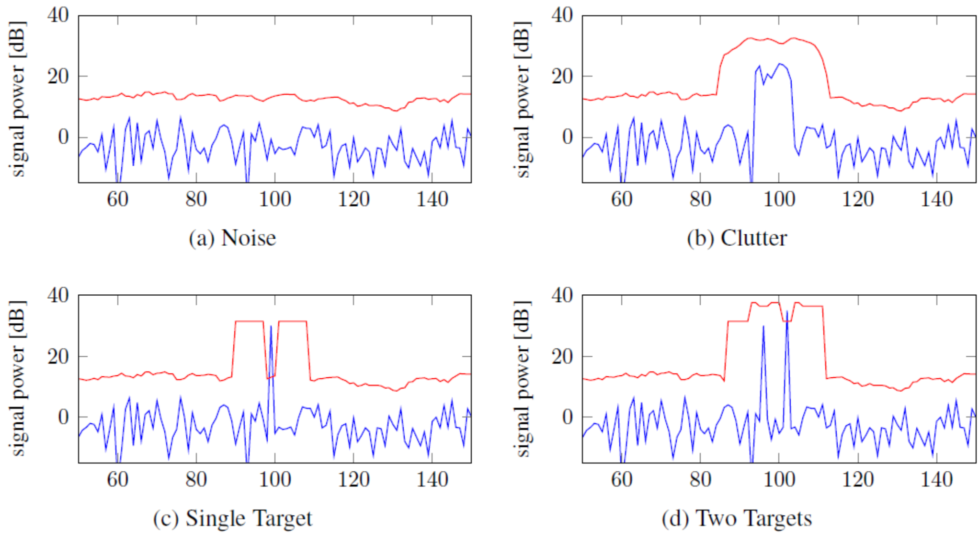

Figure 2.2.: CA-CFAR performance on a 1D signal in different signal situations (red line is detection threshold), N = 16, $P_{fa} = 10^{-6}$. Figure taken from [22]

The CAGO-CFAR shows better performance in the case of an edge between noise echoes with small amplitudes and clutter echoes with high amplitudes, yet still suffers the problem of target suppression in multiple target situations.

The CASO-CFAR shows better performance in multiple target situations, as the higher of the two means is not taken into account for computing the threshold. This only makes the suppression of a target by another target in airport ground radar less likely, yet a situation with additional targets in both the leading and lagging part of the reference cells might still occur. In such a case, the target around the CUT might still be suppressed by other targets around.

A composite method of CA-CFAR and its variations is described in 2.2.1.3.

2.2.1.2. Order-Statistics CFAR (OS-CFAR)

This CFAR method was reported by Rohling in [20] and is comprised of the theory of order statistics. In contrast to the CA-CFAR method, where all echo amplitudes within the reference cells contribute to the detection threshold, the OS-CFAR method solely selects one clutter echo amplitude the detection threshold is dependent on.

Rohling declares that it is well-known from general signal processing topics that estimation procedures are much more robust if they rest on ordered statistics [20].

All N clutter echo amplitudes within the reference window are sorted with increasing magnitude, resulting in an ordered sequence:

$$X_1 \leq ... \leq X_k \leq ... \leq X_N \tag{2.5}$$

As described before, the estimate Z for the background clutter in CA-CFAR (now denoted Z_{CA} for disambiguation) was the arithmetic mean of all clutter echo amplitudes within the reference window. For OS-CFAR, this estimate Z_{CA} is replaced by a simple rank k of the order statistic:

$$Z_{OS} = X_k \tag{2.6}$$

Rohling claims in [22] that the masking effects of CA-CFAR for multiple target situations can be completely avoided and that even weak targets in the proximity of a strong target can be detected. Furthermore, the OS-CFAR is not based on an assumption of homogeneous clutter in the reference window. This makes the detection performance less dependent on the reference window size N. The performance of an OS-CFAR scheme is shown in Figure 2.3 for different signal situations. Compared to the performance of CA-CFAR (shown in Figure 2.2), significant increases in performance in multiple target situations can be observed.

A drawback of the method is the high computational cost for ordering the clutter echo amplitudes in the reference cells. Another drawback is

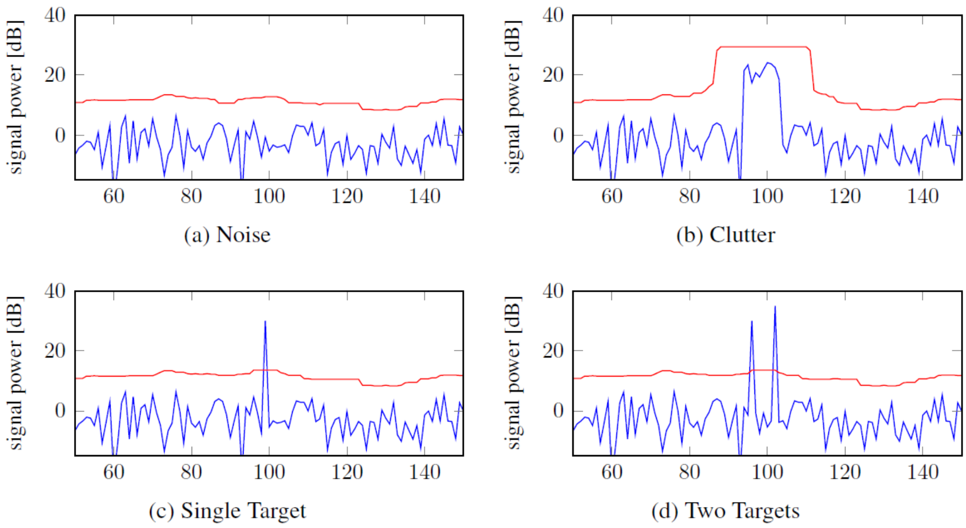

Figure 2.3.: OS-CFAR performance on a 1D signal in different situations (red line is detection threshold), N = 32, k = 24, $P_{fa} = 10^{-6}$. Figure taken from [20]

the choice of the parameter k, which has to be chosen empirically for the application data.

He [12] published a variation of the method named *Order-Statistic Greatest-Of CFAR* (OSGO-CFAR) which reduces the computational complexity, by seperatly computing ordered statistics for the leading and lagging part of the reference window, followed by a greatest-of selection.

Di Vito et al. [4] compared the performance of OS and OSGO-CFAR methods in different clutter backgrounds and found out that OSGO-CFAR shows superiority in control of false alarm probability in non-homogeneous background with clutter edges.

Due to the reduced computational complexity and the better performance in non-homogeneous clutter, the OSGO-CFAR might be a good candidate for target detection in airport ground radar. In airport ground surveillance with radar, very strict real-time requirements have to be met. This might still make a simple CPU implementation of the OSGO-CFAR method too slow, though possibilities to implement the method on highly parallelized hardware such as a GPU should be taken into account.

2.2.1.3. Variability Index CFAR (VI-CFAR)

Smith and Varshney reason that the need to accommodate a variety of environments resulted in the development of composite processors. According to them, such composite processors have the intelligence to assess the current background level and choose the appropriate estimator. They proposed a composite approach of CA-CFAR, CAGO-CFAR and CASO-CFAR (described in Section 2.2.1.1) in [23].

Variability Index CFAR(VI-CFAR) incorporates a background estimation algorithm, which estimates the background clutter power in a test cell by calculating the mean of the radar echo levels in a group of reference cells surrounding the test cell, exactly like the aforementioned CA-CFAR method and its variations. In contrast to these other methods, the VI-CFAR dynamically selects which particular group of reference cells it estimates the background clutter level from: the lagging half of the reference cells, the leading half of the reference cells, or all of the reference cells.

Therefore, this method is able to combine the advantages of CA-CFAR and its variations and achieves overall superior performance to any of its components by itself (also shown by Smith and Varshney in [23]).

The choice of which parts of the reference cells to use for the clutter background estimation, is based on the second-order statistic *Variability Index* (VI) and the *Mean Ratio* (MR) statistic. VI is defined as:

$$VI = 1 + \frac{\hat{\delta}^2}{\hat{\mu}^2} = 1 + \frac{1}{n-1}\sum_{i=1}^{n}(X_i - \hat{X})^2/(\hat{X})^2 \tag{2.7}$$

where $\hat{X}$ is the arithmetic mean for the n cells in a half reference window.

Smith and Varshney further propose a simplification of VI named VI^*, which reduces the computational load by using the biased maxium likelihood estimate instead of the unbiased variance estimate used in equation 2.7:

$$\begin{aligned} VI^* = 1 + \frac{\hat{\delta}^2}{\hat{\mu}^2} &= 1 + \frac{1}{n}\sum_{i=1}^{n}(X_i - \hat{X})^2/(\hat{X})^2 \\ &= n\sum_{i=1}^{n}(X_i)^2/(\sum_{i=1}^{n} X_i)^2 \end{aligned} \tag{2.8}$$

VI^* has to be computed separately for the lagging and leading parts of the reference window. For both of the halves of the reference cell window, a decision has to be made as to whether its cells are from a homogeneous (non-variable) or non-homogeneous (variable) environment. Therefore, the following hypothesis test is applied:

$$\begin{aligned} &VI^* \leq K_{VI} \Rightarrow non - variable \\ &VI^* > K_{VI} \Rightarrow variable \end{aligned} \tag{2.9}$$

The MR statistic is the ratio of the mean values of the reference cells in the leading half of the reference window (denoted by subindex A) and the reference cells in the lagging half (denoted by subindex B):

$$MR = \frac{\hat{X}_A}{\hat{X}_B} = \sum_{i \in A} X_i / \sum_{j \in B} X_j \tag{2.10}$$

A is defined as the set of all reference cells in the leading, B as the set of all reference cells in the lagging half of the reference window.

The MR increases if an interfering target is present in the leading half and decreases if a target is present in the lagging part. To decide if the means in the two halves of the reference window differ, the MR is compared with a threshold K_{MR} and its reciprocal:

$$\begin{aligned} K_{MR}^{-1} \leq MR \leq K_{MR} &\Rightarrow same\ means \\ MR < K_{MR}^{-1} \quad or \quad MR > K_{MR} &\Rightarrow different\ means \end{aligned} \tag{2.11}$$

The formation of the adaptive threshold based on the statistics of the VI and MR and the resulting hypothesis are depicted in table 2.1. The constants C_N and $C_{N/2}$ are calculated a priori based on the chosen probability of false alarm and the size of the reference window:

$$\begin{aligned} C_N &= (P_{fa})^{-1/N} - 1 \\ C_{N/2} &= (P_{fa})^{-1/(N/2)} - 1 \end{aligned} \tag{2.12}$$

The size of the reference cell windows can be factored into the constants C_N and $C_{N/2}$ so that the sums Σ_A, Σ_B and Σ_{AB} can be used for calculation of the adaptive target detection threshold instead of the mean levels.

Varying A	Varying B	Diff. means	Threshold	$\hat{=}$ Method
No	No	No	$C_N \Sigma_{AB}$	CA-CFAR
No	No	Yes	$C_{N/2} max(\Sigma_A, \Sigma_B)$	CAGO-CFAR
Yes	No	-	$C_{N/2} \Sigma_B$	CA-CFAR
No	Yes	-	$C_{N/2} \Sigma_A$	CA-CFAR
Yes	Yes	-	$C_{N/2} min(\Sigma_A, \Sigma_B$	CASO-CFAR

Table 2.1.: Computation of an adaptive threshold based on VI and MR of reference cell window halves A and B and the corresponding methods (adapted from [23])

The computational complexity of the procedure remains manageable and makes the method interesting for application to target detection in airport ground radar, where many different types of clutter are present and the usage of CA-CFAR or one of its variations alone is impossible. The computational complexity is also an advantage over the OS-CFAR (see Section 2.2.1.2) method, as no ordering of cells in the reference window is necessary.

A drawback is that the thresholds K_{MR} and K_{VI} have to be estimated a priori for the environment of application (described in more detail in [23]). These thresholds are vital for the performance of the VI-CFAR scheme and may lead to bad results if badly estimated.
Moreover, its detection performance will degrade considerably when interfering targets are not confined to a single half of the reference window (as Farrouki and Barkat noted in [6]).

A variation to counter this effect named *Modified Variability Index CFAR* (MVI-CFAR) has been proposed by Xu et al. [26]. If both halves of the reference cell window are thought to be varying (inhomogeneous), instead of the CASO-CFAR, a scheme named *Trimmed-Mean CFAR* (TM-CFAR, published by He et al. [13]) is incorporated. The TM-CFAR simply orders the cells in the reference windows and then trims k_1 cells from the lower end and k_2 cells from the upper end of the ordered sequence to improve robustness against interfering targets. This variation is of course computationally more expensive, as the cells in the reference window need to be ordered. The additional ordering might limit the applicability of this variation to airport surveillance with its strict real-time requirements.

Another variation proposed by Zhang et al. [27] also counters the effect of degrading performance in presence of a target not confined to one half of the reference window. This method works on ordered cells as well and so the same doubts about conformity with real-time constraints apply.

A further method based on ordered data variability has been proposed by Zhao et al. [28].

2.2.2. Temporal (Clutter Map) CFAR Detection

The sliding window principle for range-CFAR target detection works well in homogeneous clutter environments, but problems arise in inhomogeneous environments. Therefore, a method based on temporally adaptive thresholds named *Clutter Map CFAR*(CM-CFAR) has been proposed. Clutter Maps were first studied by Khoury and Hoyle [14] and Nitzberg [17].

In temporal CFAR detection, the parameters of the clutter probability distribution function are estimated by looking at echoes of radar cells in a number of scans. The methods assume that measurements of the same radar cell in two consecutive scans are statistically independent. Nitzberg reasons that this assumption holds if the radar carrier frequency is changed between consecutive scans and if the spacing between the two carrier frequencies is at least equal to the signal bandwith [17].

He also states that in case of radar with constant carrier frequency, a long enough time period between two consecutive scans is sufficient [17]. In the case of SMR surveillance for airport ground control, two consecutive measurements will typically be one second apart, such that the independence assumption holds.

As there can be a vast number of radar cells, long term storage for a number of scans can be become memory exhaustive. Nitzberg proposes computing the background estimate derived by exponential smoothing of the radar cell echoes in a number of consecutive scans to counter the high memory demand [17].

By using exponential smoothing of the radar echoes, the background estimate $Y_n(k)$ at radar scan n for radar cell k with its current measurement $X_n(k)$ would be calculated as:

$$\begin{aligned} Y_0(k) &= X_0(k) \\ Y_n(k) &= \alpha X_n(k) + (1-\alpha)Y_{n-1}(k) \end{aligned} \tag{2.13}$$

which can be rewritten to clarify the exponential smoothing effect:

$$Y_n(k) = \alpha \sum_{i=0}^{N} (1-\alpha)^i X_{n-i}(k) \tag{2.14}$$

where N denotes the number of overall observed radar scans and $0 < \alpha < 1$. By using exponential smoothing, only the previous estimate needs to be stored in memory. The *exponential smoothing factor* α defines the weight and speed of decay for old measurements in the estimation of the parameters of the clutter background probability density function.

Just as with range methods, the adaptive target detection threshold is then formed dependent of the chosen P_{fa} as:

$$T_n(k) = Y_{n-1}(k) + S \tag{2.15}$$

$$S = ln\frac{1}{P_{fa}} \tag{2.16}$$

Lops and Norsini [15] proposed that several range cells with homogeneous clutter background could be mapped into one "map cell". Within the map cell, some statistic such as a simple arithmetic mean over the echoes of the single radar cells is applied to form the current measurement. The estimate for the background clutter level in the map cell is then updated by exponential smoothing as described before. Lops and Norsini state that non-linear processing of the radar cells within a map cell (such as selecting the maximum radar echo) is more effective, as it is more robust to statistical outliers. By using map cells, the memory need for storing clutter map information can be further reduced. An obvious drawback is that the map cells have to be designed beforehand based on the homogeneity of clutter background.

Lops and Norsini [15] point out a major drawback of temporal averaging to estimate clutter background levels: the procedure suffers from performance degradation in the case of very slow-moving or fixed targets which remain in the same radar cell or map cell for several scans. In this case, the threshold progressively rises which causes the targets to ultimately not be detected anymore. This is called the *auto-masking* or *self-masking* effect.

Some methods for auto-masking avoidance have been proposed in literature, which are described in the following section.

Another way of coping with the problem is by designing Hybrid-CFAR procedures, where a Range-CFAR procedure is first applied to the cells in the map cell, followed by temporal averaging of the estimations. The Range-CFAR procedure will yield a more robust estimation of the clutter background signal level within the map cell, which results in better results. Such procedures are described in Section 2.2.3.

Auto-Masking Avoidance

A number of methods for auto-masking avoidance have been described in literature, which will be explained here.

Ferri et al.[8] propose lowering the detection threshold when a target is declared present in a map cell. This means that S in equation 2.15 is replaced by a $\delta < 0$ after a target has been declared present in the tested cell for a number of consecutive scans (Ferri et al. [8] propose to set the number to four scans). After the target leaves the map cell, the threshold coefficient has to be replaced by S again (after a number of consecutive scans in which no target has been declared present).

Conte and Lops [2] propose to censor radar signals with strong amplitudes for the computation of the target threshold. To do so, they propose not taking the average of the radar cells within the map cell, but rather taking the k-th order statistic of the map cell. This way, the $k-1$ highest echoes are filtered out.

In another publication, Conte et al. [3] propose smoothing strong radar echoes by filtering them with Ll-filters before performing a temporal average (further described in Section 2.2.3) .

2.2.3. Hybrid CFAR Detection

Conte et al. describe in [3] that hybrid CFAR methods have been proposed and validated as a suitable means for FAR regulation. They explain further that such systems are named hybrid after their operation, in that the clutter or noise distributional parameters are estimated by first processing spatial samples during every radar scan from a bunch of range cells grouped in a map cell, which are then subsequently filtered on a scan-by-scan basis (temporal averaging).

Conte et al. also state that such hybrid schemes have shown to outperform classical procedures, such as Range-CFAR or Temporal-CFAR by itself, in all practical situations if suitably optimized.

The method presented by Conte et al. in [3] first spatially filters the radar cells in a reference window by applying a so-called Ll filter to it (presented in [18]). Ll-filters form their estimate of a background signal level by linearly filtering ranked samples from a reference set, taking into consideration the rank but also the spatial proximity of the sample to the cell under test [18]. The outcome of the Ll-filter is then input to a clutter map, which then performs temporal averaging on the clutter background signals. The method yields favorable results, but unfortunately is computationally too expensive for the application of target detection in airport radar surveillance.

Another method, introduced by Ebrahimian [5] derives from Contes description at the beginning of the chapter. The method called *complex spatial / temporal CFAR* (Complex S/T CFAR) does not process radar scans first spatially and afterwards the outcome on a temporal basis. It rather processes the radar cells spatially and temporally in parallel (depicted in Figure 2.4) and forms a single detection threshold based partly on the clutter map processing and partly on the CA-CFAR scheme used for the spatial processing (thus $\alpha + \beta = 1$ for the coefficients shown in Figure 2.4). The method was designed to benefit from advantages of both methods. However, the auto-masking process for slow moving and static targets is only slowed down and still remains a problem in detecting such targets.

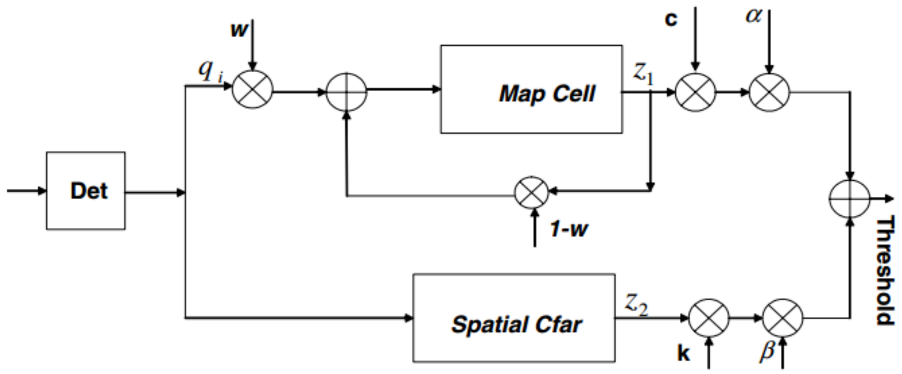

Figure 2.4.: Complex Spatial/Temporal CFAR scheme. Formation of a detection threshold partly based on spatial (β) and partly based on temporal processing (α). Figure taken from [5]

2.3. Tracking for Target Detection

Tracking in ATC surveillance applications is typically performed at a later step than target detection, when position data from different surveillance sensors is fused. However, additional tracking during radar target detection would make the detection scheme usable in a standalone manner. Target position predictions relying on the tracked object's observed trajectory could be used to extrapolate missed target detections due to short losses of radar coverage or variations in radar intensities. It is important to note that for this presented work this extrapolation of few consecutive detection misses is the main goal of adding tracking functionality to the SMR target detection scheme.

Kalman filters are very commonly used for tracking and state prediction in many fields of application (introduced in [19]).The Kalman filter works in a recursive manner (previous measurements do not need to be stored in order to estimate current and predict next state), which makes it well suited for real time applications such as the one that is the subject of this work. Many detailed explanations of Kalman filters and tutorials of high quality can be found in literature (for example in [24]), such that the reader is referred there for gaining an understanding.

Moving objects on the airport ground show different motion models (acceleration, constant velocity movements, turning maneuvers). Kalman filters are based on a single motion model, which might make tracking too inaccurate for this application. For the mentioned application, it is important that after a few missed detections the position prediction is still accurate enough to be able to match the track with a detection of the tracked object in the following time step. If only one motion model is used, even after only one or two detection misses, the difference between actual and predicted position of the track might be too large to achieve this matching.

The *Interacting Multiple Model* algorithm presented by Blom and Bar-Shalom [1] addresses tracking situations in which more than one motion model is needed. The method works with a bank of Kalman filters with different motion models and a transition probability matrix between the models. Based on how well an observed measurement fits the associated motion model of the Kalman filters, a weighed state and covariance estimate is computed. This is done in an *Interaction/Mixing*, *Filtering*, *Combination* cycle. The computational load of the method grows with the used number of models. In any case, if only used for the purpose of compensating very few consecutive detection misses, the number of models shall not surpass two to three. The application should then still be manageable in real-time and accurate enough over a duration of one or two missed detections.

2.4. Summary

In the beginning of this chapter a data analysis of available operational datasets was conducted (Section 2.1), during which a number of properties for the "targetness" of radar returns were extracted. In Section 2.2, a variation of *CFAR* methods from general radar processing were analyzed for their applicability to the application at hand. By its concept, CFAR methods should be sufficient for target detection in radar data. However, detecting targets in ground radar data by CFAR processing on signal level only (assuming all remaining radar echoes after CFAR adaptive filtering are real targets) would result in a vast number of false targets. This is due to the fact that the concept of targets on signal level and targets on meta-level (targets relevant to air traffic control) differ greatly. Therefore, CFAR processing can only take the role of a preprocessing step in the design of a target detection scheme. Due to that as well as the application being subject to strict real-time requirements, only computationally light-weight CFAR methods can be used for the design of a target detection scheme. Further processing on meta-level is needed for which the "targetness" properties defined in Section 2.1 can be used as heuristics. In Section 2.3, the usage of tracking on target detection level for extrapolation of missing target detections and improved detection results was proposed.

3. Design and Implementation of a Target Detection Scheme for SMR Data

In this chapter, the design of a target detection scheme for security-relevant targets in Surface Movement Radar Data is presented. The scheme is based on the outcome of the data analysis and literature research presented in Chapter 2. For the design of the target detection scheme, it was important to only choose methods which are computationally light and can be run in parallel in order to meet the real-time requirement of the application to airport surveillance. Furthermore, the designed scheme should be kept as generic as possible, so that it can be easily adapted for use at various airports with different radars.

To ensure compliance with the afore-mentioned real-time requirements, the target detection scheme has been modularized and designed as a pipeline to make parallel computation possible. The properties for the "targetness" of SMR echoes identified during the data analysis were followed closely and implemented to reach a high detection rate for targets and keep the false target rate as small as possible. The conceptual steps of the target detection scheme are depicted in Figure 3.1.

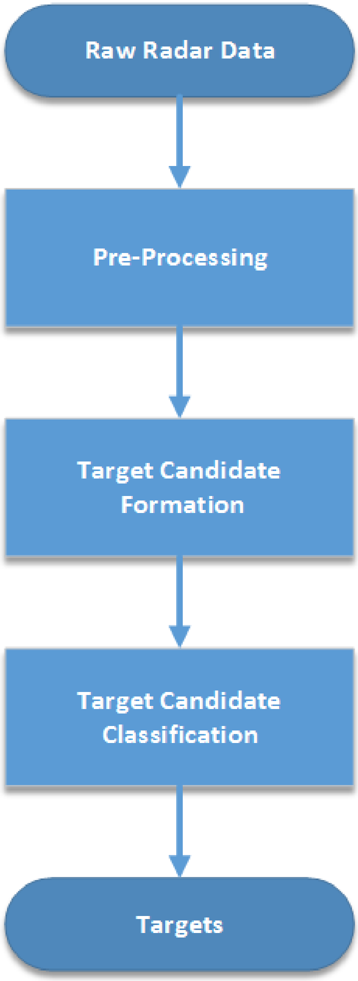

Figure 3.1.: Processing pipeline from raw radar data to extracted targets for the proposed method

The three main steps of the procedure are:

- *Radar Data Pre-Processing*: preparation of the input radar data for better target detectability in the following step
- *Target Candidate Formation*: formation of target candidates from pre-processed input data based on configurable target candidate formation method

- *Target Candidate Classification*: classification of target candidates into *target* and *non-target*, contingent on spatial and temporal properties. The definition of "targetness" defined from the data analysis (see Section 2.1) is also incorporated here.

The design of these conceptual parts of the processing chain are explained in detail in Sections 3.1 through 3.3. Details about the implementation of the conceptual detection scheme are mentioned in Section 3.4.

3.1. Radar Data Preprocessing

The first step in the target detection scheme is pre-processing of the radar data. The main goals of this processing step are a normalization of the input data, to ease the automated detection of targets in the following detection step and to visually prepare the radar video for displaying it to the user of the surveillance system. This module consists of two optional pre-processing steps, namely a data normalization and an adaptive filtering step for non-target radar echoes on signal level. Figure 3.2 shows a flow diagram of the module.

3.1.1. Data Normalization

To perform data normalization, first a histogram of radar echo intensities is formed over a number of scans. The histogram is then spread across the available dynamic range of 8-bit intensity values. In image processing, this procedure is called *contrast stretch* (described for examply by Gonzales and Woods in [10]).

One of the reasons why the radar input data should be normalized are aging effects of magnetron radars. These types of radars use strong vacuum tubes for generating microwaves of specified wavelength to be sent out for radar detection. These tubes are called magnetrons and are designed to produce waves of specified energy level. As explained in Section A.1, the ratio of received reflected energy to this specified sent out energy for any

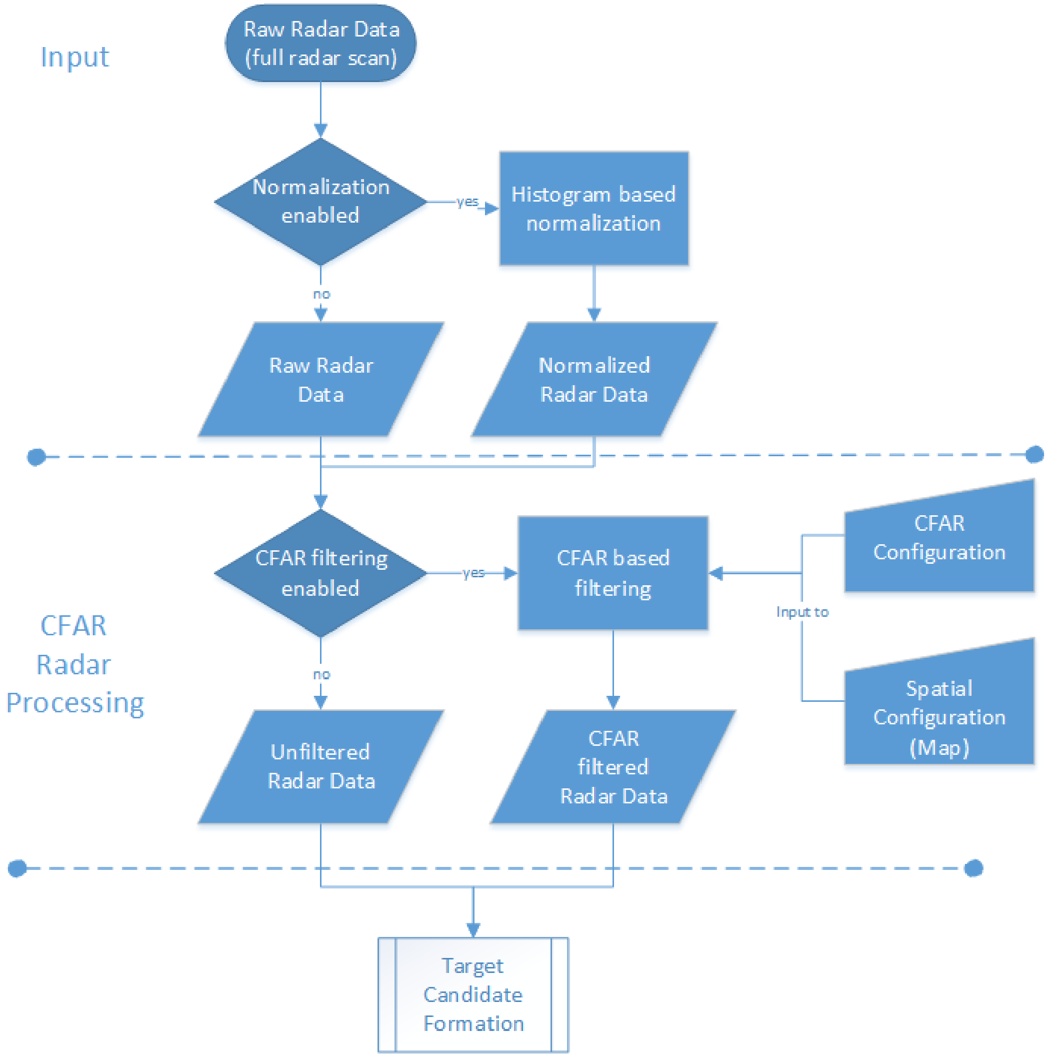

Figure 3.2.: Flow chart of Target Detection Scheme Part 1 - Data Normalization and CFAR Processing

fixed position within the radar range is digitized to represent the radar echo of this position. As the magnetron within a radar ages, the energy of the generated waves decreases. This leads to the fact that for older magnetrons the dynamic range of digitized radar echo levels is not fully used.

Another reason is that at bigger airports more than one SMR is needed to fully cover the movement areas to be surveilled. To ensure comparability between the processed output of both radars, the radar data should be normalized.

3.1.2. CFAR Processing

This processing step incorporates *Constant False Alarm Rate* (CFAR) processing (CFAR methods are explained and discussed in detail in Section 2.2, for an explanation of CFAR methodology please refer to this section).
In CFAR methodology, radar data is analyzed statistically on signal level and a decision is made as to whether an SMR echo is considered a target echo or a non-target echo by adaptively filtering the data.

As described in Section 2.4, CFAR processing only takes the role of a preprocessing step in the presented automated target detection scheme with necessary further processing steps to reduce the number of false targets. As a by-product, the CFAR processed video can be used as a filtered representation of the radar video for display in the surveillance system. Typically, the user of the system is presented with an overlay of radar video and detected targets. The CFAR processing removes noise and unwanted visual clutter from the radar video, resulting in a clearer visual representation. The user of the system hence has the possibility to toggle between raw and filtered radar video as needed.

A number of methods have been implemented (all these methods are described in detail in Chapter 2): CAGO-, OS- and VI-CFAR, Clutter Map CFAR and Hybrid-CFAR systems of Clutter Maps combined with any of the implemented range-based variants.

Figure 3.3 shows a comparison between raw and CFAR processed radar images. The method used for the CFAR processing in the sample image was a Hybrid-CFAR system with Clutter Map combined with OS-CFAR filtering. This is also the method that was later used for the experimental evaluation of the target detection scheme on operational radar data. The method was chosen because it shows superior performance to simple Range- or Temporal-CFAR methods and is computationally less expensive than more complex Hybrid-CFAR approaches.

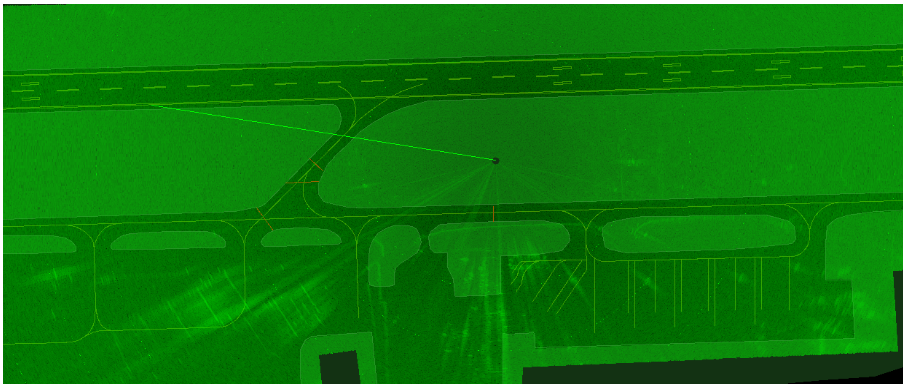

(a)Unfiltered SMR image (East-Midlands Airport)

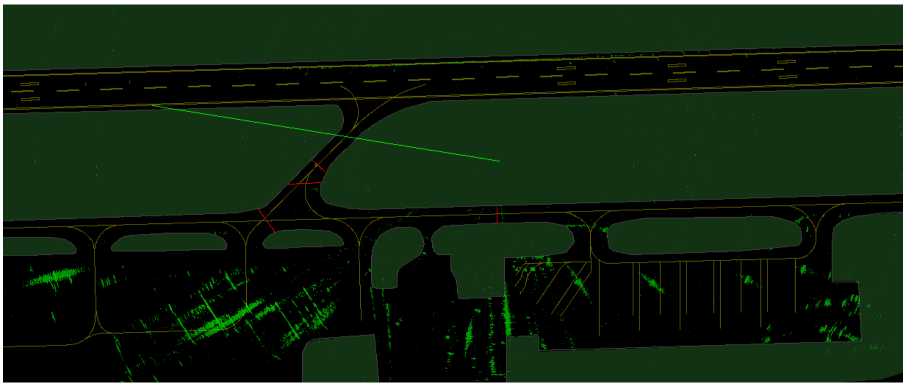

(b)CFAR filtered SMR image (East-Midlands Airport)

Figure 3.3.: Comparison between raw and CFAR-filtered SMR images

3.2. Target Candidate Formation

After the (optional) preprocessing step in which the radar data is prepared for target detection on signal level, target candidates are formed on a meta-level. For candidate formation on meta-level spatial information (such as position, size and shape of the radar echoes) and temporal information (such as target candidate trajectories) are taken into account. The results of this processing step are the positions (in cartesian coordinates) of target candidates for a radar scan, together with properties of different nature of the target candidates (eg. spatial). The target candidates are input to the classification processing stage. This stage encapsulates the logic as to which conditions a target candidate should fulfill to be considered a target relevant to air traffic control. Due to this split, the performance of the detection scheme can be measured and analyzed more easily and accurately, as more specific performance measures can be applied.

The most important performance measure for the target candidate formation step is the rate of candidate formation for true security-relevant targets. This is intuitive, due to the sequential architecture of the detection scheme. If security-relevant targets do not form target candidates, they cannot be detected by the overall detection scheme.

Based on the ”targetness” properties presented in Section 2.1 for radar targets on a signal level, a number of methods for target candidate formation were tested.

During the data analysis (presented in Section 2.1), the observation was made that security-relevant target intensities contrast from their neighboring cells. The intensities of target echoes form a local intensity maximum within their surroundings. Following this observation, methods evolving around local maxima detection on signal level were implemented. The first implemented method was a window-shrinking approach around local maxima. To form target candidates, the intensity of radar samples within a fixed size window is iteratively checked for deviation from the maxima. The starting window size corresponds to the size of the biggest target expected to be detected (ICAO aircraft category A, such as a Airbus A-380). The window around the local maximum is then shrunk iteratively as long as the "fill rate" of the window is below a configured rate. This "fill rate" was defined as the number of samples within the window that are within a configured deviation range of the intensity of the local maximum, divided by the total number of samples within the window. The method can be optimized to be very fast, it however only provides a size hint for the target candidate and does not handle targets larger than the biggest expected ATC target correctly.

To get the exact size of the target candidate, a region growing approach (described in [10]) was implemented as well. For this approach, radar samples surrounding the maximum are iteratively added to the target candidate region while they are similar in intensity. For the implementation, a configuration parameter was added which specifies the allowed deviation range from the maximum value for a radar sample to be considered similar in intensity. This also follows the contrast property identified in the data analysis in Section 2.1. This approach is slower than the window shrinking approach, as it involves more computations and iterations per maximum.

Due to the close relation and good fit with the evaluated "targetness" properties, so-called *Maximally Stable Extremal Regions* (MSER, introduced by Matas et al. [16]) were another one of the implemented methods for target candidate formation. MSERs are connected regions, which remain stable over a large number of thresholding operations. Stable means that the size of the region almost does not vary. In order for an MSER region to stay stable over many thresholding operations, the samples within the region need to be of similar intensity and be surrounded by contrasting background. As elicited in the data analysis, target radar echoes share these properties (regions of similar intensity, contrast).

Figure 3.4 below shows a flowchart for the processing step of target candidate formation. Independent of the method, information about the target is computed and stored. This information contains the candidate region, the area of the candidate region, candidate region intensities and the candidate region centroid position. In addition, the length to widht ratio of the candidate region is computed along with the metric length and width properties. Either MSER Processing or Maxima Processing is applied for the candidate formation, the paths through the flow chart are mutual exclusive.

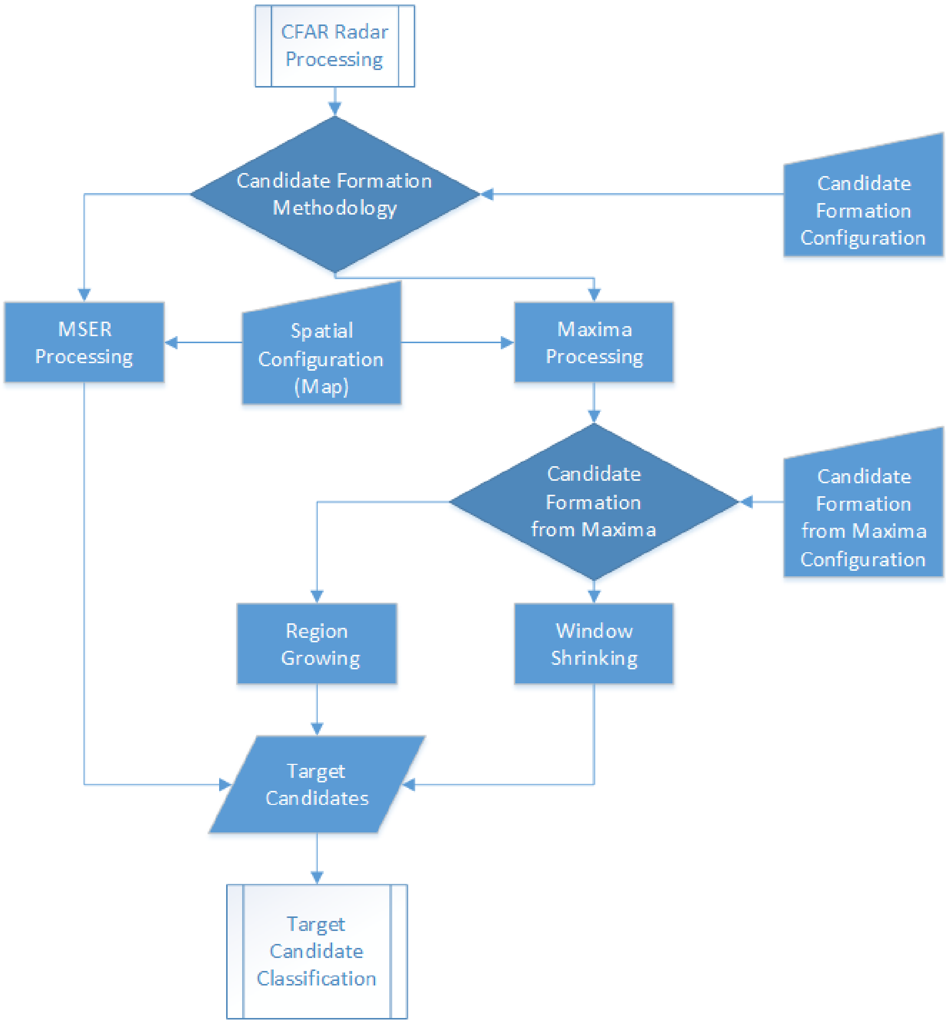

Figure 3.4.: Flow chart of Target Detection Scheme Part 2 - Target Candidate Formation. Either MSER Processing or Maxima Processing is applied

3.3. Target Candidate Classification

In this processing step, the previously formed target candidates are either verified as security-relevant targets (classified as *target*) or dropped (classified as *non-target*).This classification is the step from targets on signal level to targets on meta level (targets relevant for ATC ground surveillance).The properties on which this classification is based were elicited in the data analysis, described in 2.1. Generally speaking, the classification properties can be split into two major groups: spatial and temporal classification properties. The classification methodology derived from the elicited properties is visualized in Figure 3.5. Target candidates are sequentially checked if they fulfill the spatial and temporal properties of security-relevant targets. If a target candidate does not match the spatial properties, it can already be classified as a non-target. If the spatial properties match however, an additional check is performed to examine if the temporal properties of security-relevant targets are fulfilled. Should the temporal properties not be fulfilled, the target candidate under test is classified *non-target*. Otherwise, the candidate is classified as *target*. This means that only target candidates whos spatial and temporal properties fit the elicited model for security-relevant targets are finally classified as targets and reported to the air traffic controllers.

3.3.1. Spatial Classification

The spatial classification step checks a number of spatial properties of the target candidates. This was implemented as a pipeline, so that a number of candidates can be checked in parallel. As all of the properties need to be fulfilled, a candidate can be classified as *non-target* as soon as one check fails.

The data analysis showed that the probability of occurrence of security-relevant targets is dependent on the location of the radar echoes on the airport. Security-relevant targets are expected with higher probability in *Movement Areas* of the airport compared to other airport areas (see Section 2.1 for details). As a result, a labeled airport map was introduced to incorporate locality information. This lookup map has the same size as the output image of the radar in use and classifies every pixel of the output image into *Movement Areas* and *Non-Movement Areas* (for description of the area types, refer to Section 2.1). A switch was added in configuration, which determines how target candidates in *Non-Movement Areas* should be handled. One setting for the switch is to immediately classify target candidates in *Non-Movement Areas* as *non-target*, without further investigations.

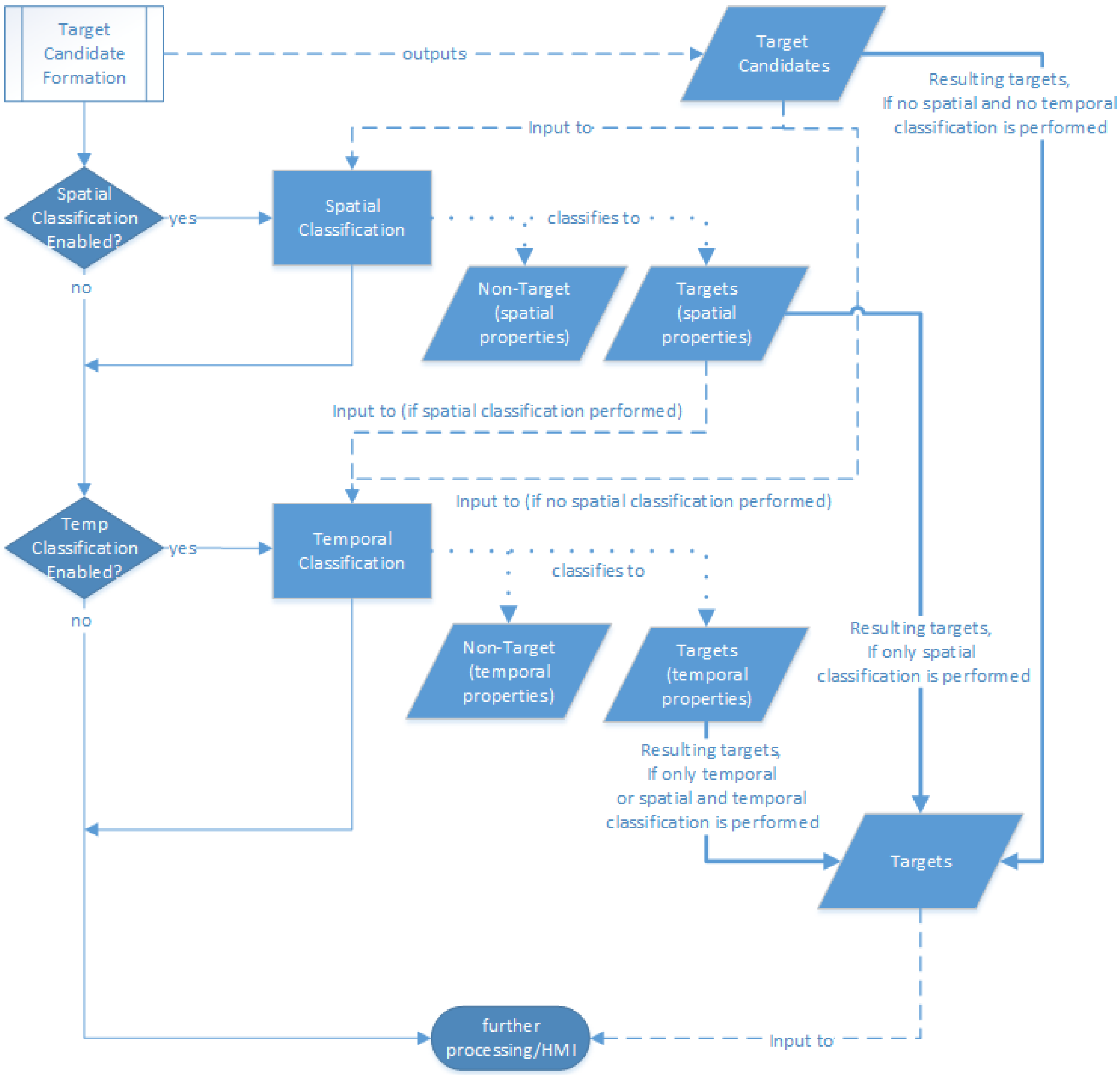

Figure 3.5.: Flow chart of Target Detection Scheme Part 3 - Target Classification

The other possible setting is to only attenuate the target candidate with the information that it lies within a *Non-Movement Area* and continue with the classification chain, in a way that the candidate might end up being classified as *target* in the end. The configuration parameter was mainly introduced to give the operator the possibility to decide whether targets in *Non-Movement Areas* should be detected and visualized or not.

The first checked property is the maximum intensity of the target candidate. This check is done to filter target candidates obviously induced by noise with very low maximum intensities, which might otherwise result in false targets.

Next, it is checked if the size of a target candidate lies within the range of size for expected security-relevant objects. The length, width and area of a target candidate are all checked separately. These checks are done in the metric system, such that the size of the target candidate area has to be calculated depending on the distance from the radar (as radar sample size increases with distance from the radar; for details about radar image formation see A.1). The lower threshold for the size of expected security-relevant objects is constrained by the radar resolution, which typically is between three and seven meters. The upper thresholds for area, length and width were set to the dimensions of the largest expected security-relevant object (very large aircraft, such as an A-380).

During the data analysis, an observation was made that very often concrete curbs at borders of taxi- or runways produce very strong radar echoes. This specific case of non-security-relevant targets can be identified and filtered when looking at the length/width ratio of a target candidate region. The concrete curbs produce very elongated and thin candidate regions with very large length/width ratios, while security-relevant objects show lower length/width ratios.

It was decided to incorporate the location information into the above mentioned checks of spatial properties. Similar to the specification of *Movement* and *Non-Movement areas* within the aircraft map, parameter areas for spatial classification can be freely defined. These parameter areas may then be associated with different parameters for the spatial classification. This means that for the above mentioned checks of intensity, length, width, area and length/width ratio different limits may apply, depending on the location of the target candidate. The areas were added to gain more flexibility and be able to handle specifics of some areas of the airport.

3.3.2. Temporal Classification

In the temporal classification step, target candidates are analyzed and classified based on the temporal progression of their position. During the data analysis, it was discovered that the trajectory of radar echoes is important for classification between security-relevant and non-security-relevant targets. However, it was also discovered that a robust matching of radar echoes across radar scans is quite problematic due to low spatial resolution, changing shapes and possibly changing echo intensities. Additionally, depending on the trajectories or *tracks* of objects, a second classification into static and moving targets is performed. This allows for a more granular result of static and moving security-relevant targets.

To reduce the number of false targets which are induced from noise in the radar data, target candidates are only classified as target and reported by the detection scheme once they have been detected for a number of consecutive scans. This is called the *track initiation* process. During track initiation, target candidates can form new *track candidates* or be matched with existing ones. After the configured number of consecutive detections, a *track* may be formed from a track candidate. Any detection of a tracked target is then reported in following scans.

Algorithm 1 describes the detailed temporal classification procedure in pseudo-code. The following paragraphs describe the sequential steps from first detection of an object to the tracking of an object and explain the details.

Algorithm 1: Temporal Classification Pseudocode

```
Input:
  • Set of Target Candidates for current scan, TargetCandidates
  • Set of Object Tracks, ObjectTracks
  • Set of Track Candidates from earlier scans, TrackCandidates

Output:
  • Set of Targets (classified as security-relevant), Targets
  • Updated Set of Object Tracks, ObjectTracks
  • Updated Set of Track Candidates, TrackCandidates

for target_candidate ∈ TargetCandidates do
    if ∃track ∈ ObjectTracks and target_candidate can be mapped then
        UpdateObjectTrack(track, target_candidate);
        Classify(target_candidate, TARGET) ;
    end
    else if ∃track_candidate ∈ TrackCandidates and target_candidate
    can be mapped then
        UpdateTrackCandidate(track_candidate with target_candidate);
        if track_candidate to be promoted to object track then
            Track track;
            track = initiateTrackAndClassify(target_candidate,
            track_candidate);
            // see pseudocode listing 2 ;
            ObjectTracks += track;
        end
        else
            Classify(target_candidate, NONTARGET) ;
        end
    end
    else
        TrackCandidates += newTrackCandidate(target_candidate);
        Classify(target_candidate, NONTARGET) ;
    end
end
housekeepExpiredTrackCandidates(TrackCandidates) ;
predictPositionsOfTracksWithoutUpdates(ObjectTracks) ;
```

Track Initiation: Establishment of Track Candidate

When a new object appears in the surveillance area, a corresponding target candidate is generated after the radar scan. If the candidate passes the spatial classification, it then reaches the temporal classification step.

As this is the first occurrence of the object in the surveillance area, there is no existing track or track candidate for the object. The target candidate is therefore classified as non-security-relevant during this first detection, but is stored as a track candidate for the next scan. This refers to the section in the pseudo-code starting at line 18.

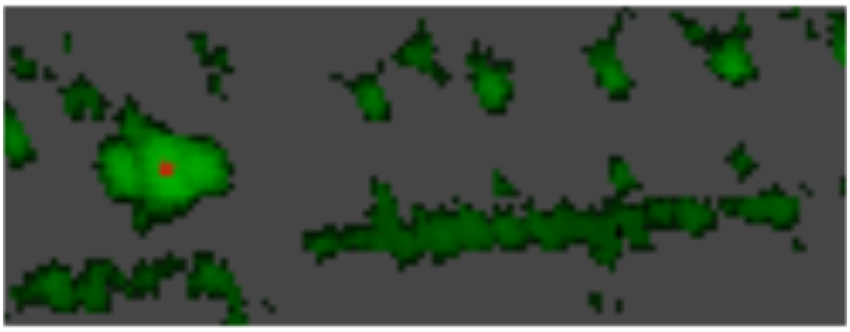

Figure 3.6.: Target candidate, after spatial processing. Centroid of target candidate region is shown in red.

As described before, during target candidate formation for each candidate a number of properties are calculated and stored. These properties will become important for the track candidate in the next scan and are therefore adopted by the track. One of these properties is the candidate region centroid. A schematic visualization of a target candidate and its centroid is shown in Figure 3.6.

Track Initiation: Matching of Target Candidates with Track Candidates

As the object is detected for the second time, a corresponding track candidate already exists, which was generated after the first occurrence of the object. However, the target candidate has to be matched with this corresponding track candidate first. To check for a match between the entities, a number of properties need to be checked. This is done in a loop over all existing track candidates to see if any one of them can be matched with the current target candidate. Data analyis showed that shapes of objects change across radar scans, such that an automatic matching based on the radar echo shape is not possible. As the resolution of the radar is quite low, a similar size of the object (number of pixels) paired with similar length and width can be seen as an approximation to the object shape. For this purpose, similarity of a property was defined to fulfill an equation of the form

$$lower\_bound \leq value \leq upper\_bound$$

The values for $lower\_bound$ and $upper\_bound$ are dependent on the checked property of one entity, while $value$ refers to the value of the checked property of the other entity. A target candidate matches a track candidate if it is similar in all checked properties. An example for such an equation set is shown below:

$$\begin{aligned} 0.9Area_{TrackCandidate} &\leq Area_{TargetCandidate} &&\leq 1.1Area_{TrackCandidate} \\ 0.8Width_{TrackCandidate} &\leq Width_{TargetCandidate} &&\leq 1.2Width_{TrackCandidate} \\ 0.9Length_{TrackCandidate} &\leq Length_{TargetCandidate} &&\leq 1.1Length_{TrackCandidate} \end{aligned}$$

The similarity factors are only exemplary; for the target detection scheme these factors were made configurable. For the reference setup, these values were tuned from sample data.

Additionally, the distance between the entities must lie within certain bounds for a possible match between them. Figure 3.7 illustrates a sample situation for a target candidate. Its corresponding track candidate from the

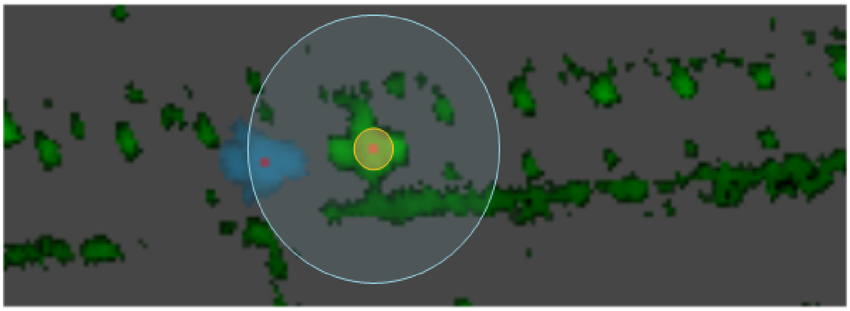

Figure 3.7.: Matching between target candidate and track candidate based on static configuration (distance circles in orange and blue)

previous scan is shown in blue as an overlay to the radar image of the current scan. The circles around the target candidate in Figure 3.7 schematically visualize configurable distance boundaries for the matching process. If a track candidate can be found within the orange circle and all equations are fulfilled, then the track candidate can be matched with the track candidate. Furthermore, the track candidate is to be considered static. On the other hand, if a matching track candidate is found within the bounds of the blue circle, the track candidate is considered to be moving. As the update rate is known and constant, this maximum distance can be statically set according to the largest expected velocities of objects (starting and landing aircraft). Any track candidates outside the blue circle are not considered at all for the matching process. It is important to note, that the closest track candidate is matched in case more than one track candidate could be matched.

A target candidate that is matched with a track candidate is still classified as non-security-relevant, as there is not yet enough information about the progression of the object's location. However, the position of the matched target candidate is stored with the track candidate. Any target candidate that cannot be matched with a track candidate will generate a new track candidate.

Tracking: From Track Candidates to Tracks

After a configurable number of consecutive radar scans during which a target candidate could be matched with a track candidate, it is safe to initiate a track from the track candidate. As the position data for the matched target candidates during each scan was stored with the track candidate, it is possible to now estimate the velocity and acceleration vectors of the object. To be able to get an estimate of the object's acceleration, it takes at least three consecutive detections of the object during which it was matched with the same track candidate to initiate a track. This is illustrated in Figure 3.8. The number of scans before track initiation can be configured to a higher number to get better estimates, with the downside of a longer delay until targets are reported first.

Once a track is initiated, any target candidate that can be matched with the track in following scans is classified as a target and reported. A number of commonly used methods for the tracking of detected targets in radar data have been explained in Section 2.3. The method which was implemented for this work is a *Interacting Multiple Model (IMM) Kalman Filter* (for details refer to Section 2.3).

As the computational load rises with the number of models used for the IMM, it was decided to restrict the number of models to two. The used models are the *constant velocity* and *constant acceleration* motion models. The initial state vectors and probabilities for the motion models of the tracks are set according to the estimated properties from the detections during track initiation.

To reduce the computational load further, Kalman filters are only used for moving tracks. Static tracks are solely tracked based on their position during the previous scan, using the static search-window also used for matching between target candidates and track candidates (orange circle in Figure 3.7). Static tracks can additionally be configured to be filtered (classified as non-target) based on locality information. This allows dynamic filtering by the user by specifying map regions for which no static objects should be reported as targets. This is useful in cases where the user knows about a static target, but does not want it to create target reports every scan (for example long-term parked aircraft). This is also shown in algorithm 2, starting at line 6.

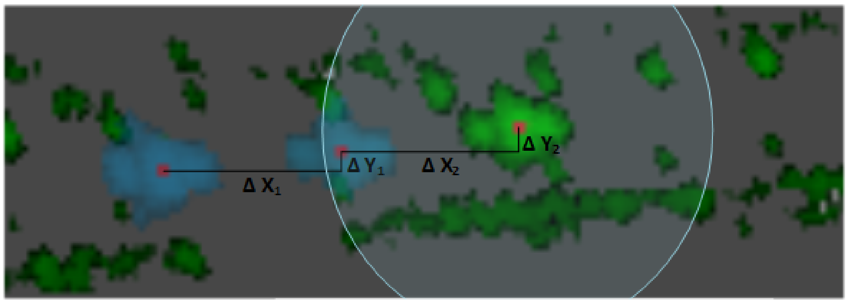

Figure 3.8.: Track candidate after third consecutive matching with target candidate. Velocity and acceleration vectors can be estimated.

Algorithm 2: From Track Candidates to Tracks

```
Input:
  • Target candidate mapped with the track candidate in scan,
    target_candidate
  • Track candidate to initiate track from, track_candidate
  • Map configuration for target detection, config

Output: Initialized track, track
Function initiateTrackAndClassify(target_candidate,track_candidate)
    Classify(target_candidate, TARGET) ;
    if EstimateMotionModel(track_candidate) == "Moving" then
        track.kalman = InitiateKalmanTrack(track_candidate) ;
        /* Initiate Kalman with inital state according to
        estimated properties of track candidate                */
    end
    else if EstimateMotionModel(track_candidate) == "Static" then
        if config.classifyStaticTargetsBasedOnLocality then
            if config.isInSurpressRegion(track_candidate.centroid) then
                Classify(target_candidate, NONTARGET) ;
            end
        end
    end
end
```

Tracking: Matching of Target Candidates with Tracks

Once a track for an object is established, the problem of associating target candidates still exists but becomes a little easier than in the case of matching with track candidates. In the case of moving targets, a modified Kalman filter is used for tracking, which works in a predict/update cycle. Determined by the prediction value of the next position of the target and the uncertainty of this prediction (covariance), a dynamic search window for target candidates in the scan can be generated. An example of this is shown in Figure 3.9. In case of a static target, the same procedure as when matching with a track candidate is applied.

Tracking: Tracks without Updates

In case no target candidate can be matched to an existing moving track, for a number of scans missed detections are extrapolated (see algorithm 1, line 23). There is a trade-off between losing tracks because of only a few missing updates and artificially adding position updates to tracks whos lifetime actually ended (because they left the surveillance or took off in case of starting aircraft). If a track is lost, the track initiation process will start again and cause a delay until the object will be detected as target again. To avoid this, an extrapolation of missing target detections becomes very reasonable. The number of extrapolated missing detections was set to at most two, which proved to be a good compromise as this also only minimally prolongs the lifetime of dead tracks.

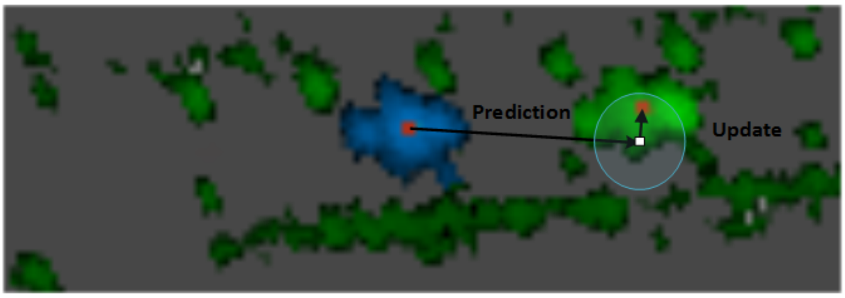

Figure 3.9.: Kalman Track, Predict/Update Cycle

3.4. Implementation Details

The designed processing scheme for target detection in ground surveillance radar in airport environments was implemented in MATLAB for rapid prototyping and detailed evaluation. The VLFeat toolbox was used for utility image processing methods. The EKF/UKF toolbox of Aalto University was used for implementation of IMM Kalman filters in MATLAB.

Furthermore, the designed processing scheme was integrated into the existing A-SMGCS solution of AviBit Air Traffic Solutions and was implemented in C++, using the Qt framework.

4. Experimental Evaluation on Real-World Datasets

Alongside the design and implementation of a target detection scheme for airport surveillance radars, the construction of a suitable evaluation method to measure detection performance was another important topic of this thesis.

Airport surveillance radar data is needed and is the key to being able to measure this performance. The cooperation partner of this work, AviBit Air Traffic Solutions, provided access to their radar setup at Bucharest Otopeni Airport, which made it possible to get this needed application radar data. The reference radar setup at Bucharest Airport is described in detail in Section B of the Appendix.

Evaluation of the performance of an SMR sensor is a difficult task. Due to the nature of the SMR sensor data, it is almost impossible to identify which object produced a certain radar echo. As defining a single evaluation method to confidently measure the overall performance of the target detection scheme is not possible, different performance aspects were measured by incorporating three evaluation methods:

- *Performance for critical traffic situations:* to measure the performance of target detection during critical traffic situations, sequences of such traffic situations were analyzed. The critical situations covered are starting and landing aircraft. The sequences were annotated with ground truth information and the detection rate and false-target rate were computed for these sequences.
- *Detailed performance analysis for small targets:* early tests showed that the hardest part for target detection was to detect targets which generate small radar echoes due to the low resolution of the radar sensor.

As described in Section A.1 of the Appendix, the spatial resolution decreases with growing radial distance to the radar. For that reason, as a worst-case analysis, a car of the airport staff at Otopeni Airport was used to perform a test drive covering all movement areas of the site. This vehicle can be seen as the smallest moving object to be detected by the target detection scheme. The recordings of this drive were then analyzed and the detection rate was computed.

- *User-experience test, long term evaluation:* to test the user acceptance of the target detection performance, a long-term evaluation by ATCOs at Otopeni Airport was set up. The system output of the ground surveillance system, including the target detection scheme, was monitored closely by experienced ATCOs and malfunction or poor performance was reported. This monitoring and reporting was done for a period of two weeks. This long-term evaluation also had the function of detecting performance problems that were missed by the previous evaluation methods.

The evaluation methods and their results for the reference setup at Otopeni Airport are described in detail in the following sections.

4.1. Performance for Critical Traffic Situations

As a first step in the evaluation process, the performance detection scheme for critical traffic situations was analyzed. More specifically, the detection rates of starting and landing aircraft of different types was evaluated. These situations are especially critical, as non-detection of starting or landing aircraft may in the worst case lead to fatal consequences in case of other objects which form obstacles on the runway. Therefore, it is vitally important that the target detection scheme works robustly in these situations for the detection of the aircraft. Additionally, it is also important that the rate of detected false targets is low for these situations. Especially along the runways lots of metallic objects are situated, which cause high-intensity radar echoes (for example runway guidance lights, see 4.1). These objects should not be detected as targets, as they do not pose a threat for a starting or landing aircraft.

For a day radar outputs of everyday-operation at Bucharest International Airport were monitored to collect test data for starting and landing operations. A number of sequences were extracted from the recordings for both starts and landings of different types of aircraft for analysis. These sequences were then annotated with ground-truth information (the visible security-relevant targets in the sequence). The sequences were then used as input for the target detection scheme and the detected targets were compared with the ground-truth labeled data.

Overall, thirty eight ground-truth annotated sequences of starting and landing aircraft were used to evaluate the performance for these situations. Twenty sequences showed landing aircraft and eighteen showed starting aircraft of different types. The number of radar scans within the sequences was about twenty, dependent on the length of the operation. A sample landing sequence is depicted below in Figure 4.1.

The results of the comparison between the output of the target detection scheme and the ground-truth annotation are shown in Table 4.1 for aircraft landings and Table 4.2 for aircraft starts.

Index	Description	Detection Rate	False Detections
1	Initial Analysis	**97.30** %	1.09 per image
2	Problematic false target removed	**99.24** %	0.85 per image
3	Dynamic suppression areas applied	**99.57** %	0.03 per image

Table 4.1.: Results of detection analysis for landing aircraft (Runway South)

For the initial analysis (1), static target suppression areas (explained in Section 23) were added along the runways, to suppress target detections for the large numbers of false targets there. The initial analysis resulted in a detection rate for the aircraft of 97.30 percent and a false target rate of 1.09 false targets per image. When analyzing the results, it showed that the false targets did not confine to the edges of the runway only. This is visualized in Figure 4.2, where false targets appear in the middle of the runway. The strong radar echoes leading to the target detection could be induced by reflections. Another possibility is that water puddles on the runway caused the strong radar echoes leading to the detection. One of the false targets was

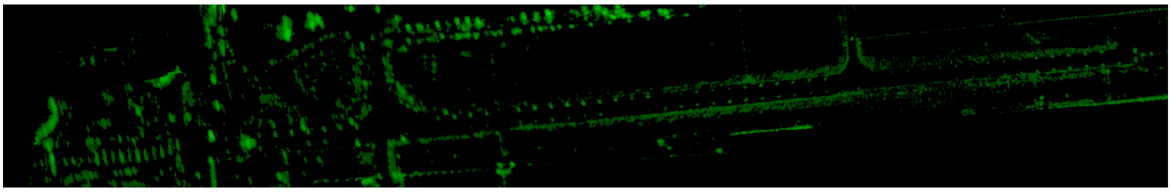

(a)1st radar scan

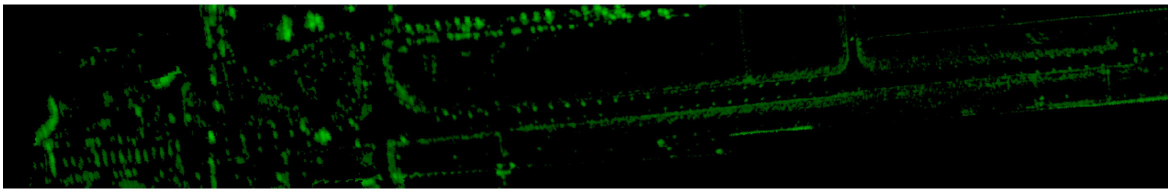

(b)5th radar scan

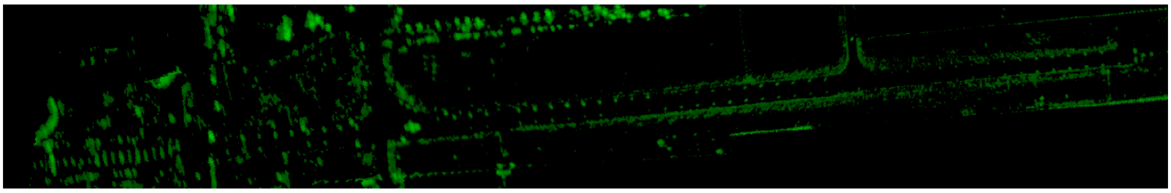

(c)10th radar scan

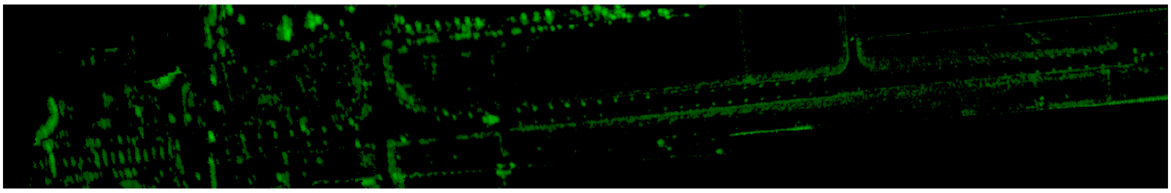

(d)15th radar scan

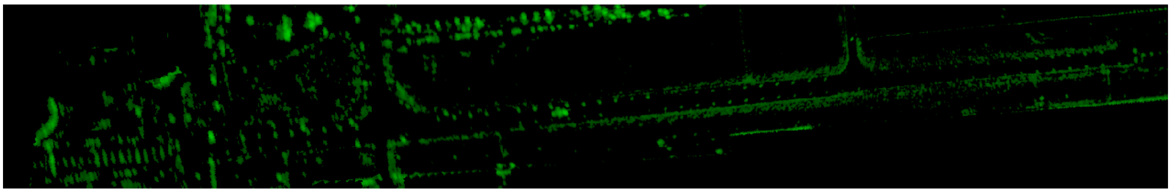

(e)20th radar scan

Figure 4.1.: Sample radar data sequence of a landing aircraft

even more problematic, as it caused missed detection of the landing aircraft (the leftmost false target in Figure 4.2). As it is situated on the very beginning of the runway, where landing aircraft first appear in the surveillance area, the false target interfered with the track initiation process of the target candidate of the aircraft. As the false target is positioned in a Movement area, shows high-intensity radar echoes contrasting with its surroundings and passes the spatial and temporal classification (as static target), it cannot be distinguished between security-relevant and non-security-relevant object correctly in that case. What is needed in this case is a manual intervention by the air traffic controller. In cases when such targets appear, it needs to be visually checked by an airfield operator. The operator may then verify the target as a false target induced by radar phenomena or a real obstacle which needs to be removed. Therefore, a possibility was added to dynamically add suppression areas within which no track initiation may be performed. When masking out this problematic false target in this way, a result of 99.24 percent detection rate, paired with 0.85 false targets per image was reached. The false target rate can be reduced to almost zero false targets per image when masking all of the (static) false targets within Movement areas, while achieving a detection rate of 99.57 percent.

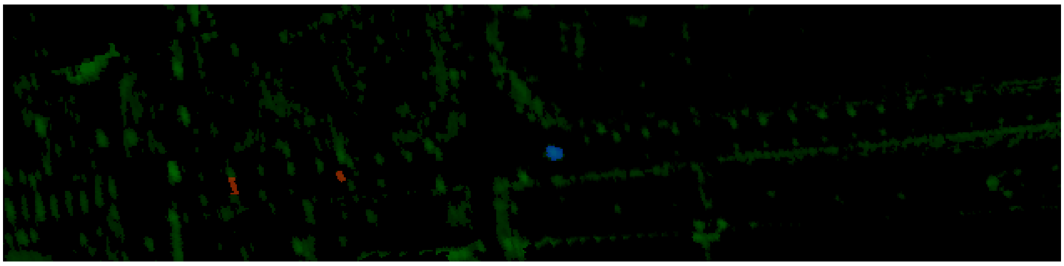

Figure 4.2.: False targets on Runway South during analysis of landing aircraft. Moving targets indicated in blue (landed aircraft), static targets in orange (false targets)

The analysis showed, that regular manual intervention is needed in order to ensure good performance of the target detection scheme. These types of false targets are induced by the nature of radar as a sensor, as all reflective surfaces will produce high radar echoes. Air traffic controllers will have to manually mask such areas and also remove those masking areas again, in case the false target disappears. When this maintenance of suppression areas is done accordingly, good results can be achieved (Analysis 3 in Table 4.1).

The results for starting aircraft are shown in Table 4.2. Already with the initial analysis, using default settings and the map for Movement/Non-Movement areas, a detection rate of 100 percent was achieved. The reason for this is that the two runways at Bucharest Otopeni Airport are operated in a manner that one is used for start operations, while the other one is used for landing operations. During the data collection process the less cluttered Runway North was used for departing flights. The radar returns are visualized in Figure 4.3, which appear a lot less affected by by effects such as the ones depicted in Figure 4.2 for Runway South.

Index	Description	Detection Rate	False Detections
1	Initial Analysis	**100 %**	0.043 per image

Table 4.2.: Results of detection analysis for starting aircraft (Runway North)

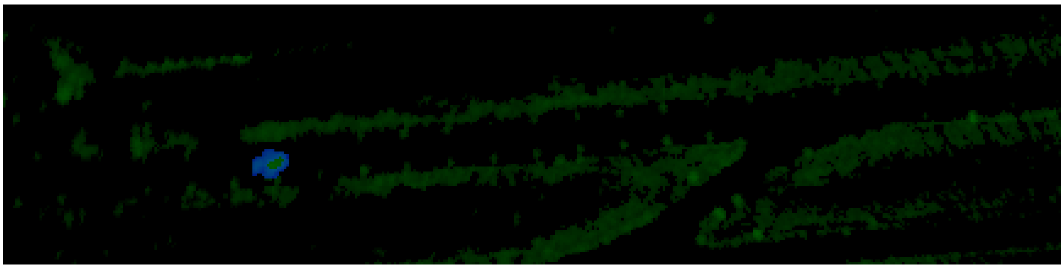

Figure 4.3.: Radar returns at Runway North during evaluation of detection scheme performance for starting aircraft

4.2. Performance Analysis For Small Targets

As stated before, the performance of a target detection scheme for SMR data is difficult to evaluate. One of the main reasons for this circumstance is the fact that by only looking at the radar echo, it is almost impossible to determine which real world object generated it. If an evaluation environment can be generated where the real world object creating an SMR echo is known, then this problem can be avoided.

To achieve this, a car of the local technical staff at Bucharest Otopeni Airport was equipped with an *Automatic Dependent Surveillance-Broadcast* (ADS-B) transponder. ADS-B is a surveillance technology for tracking object movements based on satellite navigation. An ADS-B transponder broadcasts the position of the object it is attached to at set intervals on specified frequencies. For the evaluation, the ADS-B equipped car was driven along all taxiways and runways which were of interest for target detection at the site. This was done while the target detection scheme was running. The raw radar data as well as the extracted radar targets from the timespan of this "test drive" were recorded and archived for analyzing purposes. By configuring the ADS-B transponder with an adequate localization frequency, a ground truth of the track of the car could be established. The ADS-B positions were then converted from the WGS-84 coordinate system into system coordinates used by the target detection scheme for comparability.

The route of the test drive along the movement areas of Bucharest Otopeni Airport is visualized in green on a map of the site in Figure 4.4.

Theoretically speaking, there should be a detected target corresponding to the car in proximity of the ADS-B position at every radar revolution and this coverage analysis could be done automatically. Unfortunately, this only works in theory. As ADS-B is based on GPS navigation, it achieves an accuracy of about five to seven meters. The radar's positioning accuracy decreases rapidly with radial distance of the target to the radar, such that the deviation between the two positions can become quite large. As the test drive was done during regular airport operation, this could result in false correlations of detected targets and ADS-B positions. Other objects in proximity of the ADS-B positions could have also created a target report

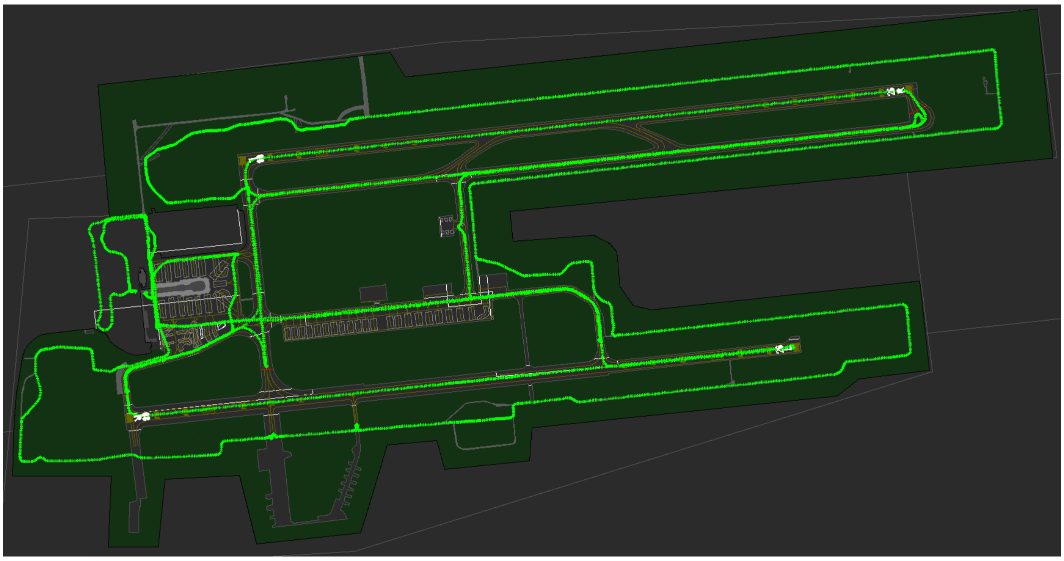

Figure 4.4.: Visualized route of the performance evaluation and coverage test at Bucharest Airport (in green)

and could be falsely correlated.

As a result, it was decided that the correlation between ADS-B positions and targets created by the test object should be done manually. Based on the ground truth and a visualization of the detected targets on the airport map, the targets created by the driving car were picked out for further analysis. Since the duration of the test drive (about 90 minutes) and the update rate of the radar sensor (one second) are known , the expected number of detections of the test object can be calculated.

For the evaluation, time spans during which the test object was stopped were excluded from the analysis. This happened, for instance, when the test object was stopped while waiting at stopbar for crossing traffic. These time spans would prolong the real duration of the test drive and artificially improve the result of the test drive.

The number of expected targets extracted for the test object can be calculated as

$$\mathbf{Num}_{\mathbf{ExpectedTargetDetections}} = \frac{\mathbf{TestDriveDuration}_{\mathbf{Adjusted}}}{\mathbf{SensorUpdateRate}} \tag{4.1}$$

and finally the *probability of detection* is calculated as

$$\mathbf{ProbabilityofDetection} = \frac{\mathbf{Num}_{\mathbf{TargetDetections}}}{\mathbf{Num}_{\mathbf{ExpectedTargetDetections}}} \tag{4.2}$$

The test drive was evaluated and analyzed on different levels. First, the *probability of detection* (PD) without incorporating temporal information was calculated. The results are shown in Table 4.3.

Index	Radars / Method	Prob. of Det.
1a	SMR East only, Untracked, Phys. covered areas only	**88.97 %**
1b	SMR West only, Untracked, Phys. covered areas only	**91.31 %**
2	Both radars, Untracked, All Movement Areas	**94.37 %**

Table 4.3.: Results of probability of detection analysis for test drive without incorporating temporal progression of target

Time spans during which the test object was located in areas without physical radar coverage were excluded from the probability of detection analysis of the single radars when not incorporating temporal information. If areas without radar coverage were to be left included in the analysis, this would worsen the result even though the missing radar coverage makes a target detection impossible. Only when taking into account information about the objects trajectory and hence the temporal progression, detections can be extrapolated. A lack of physical radar coverage can, for example, occur if the line-of-sight from radar to an object is blocked or *shadowed* by buildings or other tall obstacles. The excluded time spans were identified based on the ADS-B reference positions of the test object and information about areas without physical coverage for the radars. This information was provided by the radar manufacturer and is depicted in Figures B.2 and B.3 in the Appendix. The methods used were a Clutter Map CFAR with OS-CFAR and anti-masking effects, followed by maxima-based region growing as target formation followed by a target classification based on spatial properties only.

As the analysis for the single radars SMR East and SMR West showed, the areas without coverage are larger than shown in the coverage visualizations provided by the manufacturer. Moreover, the intensity of the radar echo of the test object showed a very large variance over the course of the test drive. In many cases, the intensity became so low, that the target candidate corresponding to the test object was classified as non-target. The results for the single radars of 88.97 and 91.31 percent probability of detection are insufficient for surveillance of airport ground movements.

If the target detections of both radars are combined for the test drive, the result is a probability of detection of 94.37 percent. To combine the results, for each of the radars an ”area of responsibility” is defined (which may overlap). Within these areas, target detection is performed separately for both radars as before. In overlapping areas a detection of the test object by either of the radars is counted as a detection. Otherwise, in case of ”single responsibility”, only a detection by the responsible radar is counted as a detection of the test object.
The result shows that the joint coverage improves the results of the single radars, which is in line with the purpose of using more than one radar to jointly cover all airport movement areas (to make up for ”blind spots” caused by occlusions). However, the analysis also showed that there are areas on the airport ground which neither of the radars cover. This is visualized in Figure 4.5, in close proximity to SMR-West the test object could not be detected as it was within the radars dead-cone (the white circle in the figure). Moreover, also SMR-East does not provide physical coverage for this area (see Figure B.3 in the Appendix).

There were also areas for both radars where the echo intensity of the test object was very low, causing the corresponding target candidate of the test object to be classified as non-target.

The PD analysis was then done again, this time incorporating information about the test objects trajectory in the detection scheme. This was done in the form of the temporal classification scheme presented in Section 3.3.2, which uses IMM-Kalman filters with constant velocity and constant acceleration motion models for location estimation. The results for the analysis are shown in Table 4.4.

Index	Radars / Method	Prob. of Det.
3a	SMR East only, Tracked, All Movement Areas	**92.85 %**
3b	SMR East only, Tracked, Phys. covered areas only	**95.68 %**
4a	SMR West only, Tracked, All Movement areas	**84.34 %**
4b	SMR West only, Tracked, Phys. covered areas only	**93.51%**
5a	Both Radars, Tracked, All Movement Areas	**97.11 %**
5b	Both Radars, Tracked, Covered Movement Areas	**99.51 %**

Table 4.4.: Results of probability of detection analysis for test drive, taking temporal progression of target into account

The analysis was done multiple times. Analogous to before, first the target detections of the single radars were analyzed. This time, the analysis for the single radars was performed for both physical coverage areas and the complete surveillance area (all movement areas of the airport). As the results of the analysis for SMR East show, incorporating information about the target trajectories brought a significant increase in probability of detection and hence performance. If only the physical coverage areas are taken into account, the probability of detection increased from 88.97 percent(1a) to 95.68 percent(3b).

For SMR West, the probability of detection within the physical coverage areas only increased from 91.31 percent(1b) to 93.51 percent(4b). The large difference in improvement between the radars can be explained when analyzing the patterns of missed detections for the two radars. Looking at the results of analysis 1a for SMR East, it shows that the radar echoes of the test object vary greatly across scans and become quite low at times. This causes many "short" missed detections, where the test object was not detected for one or two consecutive scans and was then detected again. This is exactly the situation where an extrapolation of target positions based on previously observed movements works well. Even though the detections are missing for one or two scans, the target position can still be reported based on predictions of the Kalman tracker without too much loss of precision. On the other hand, when looking at analysis 1b for SMR West, most missed detections within the physical coverage areas lasted for many consecutive scans. As stated in Section 3.3.2, a target position prediction without update is at most done for two consecutive scans, for reasons of prediction precision and artificial prolongation of track lifetime of objects no longer in the surveillance area. Hence, in this case the tracking of target positions cannot improve the result by much.

Finally, the probability of detection was again analyzed when joining the detections of both radars. For analysis 5a, the probability of detection for all movement areas where the test object drove during the test was taken into consideration. For this analysis, a probability of detection of 97.11 percent was calculated. As stated before, a number of areas were identified which neither radar had phyisical coverage for and which where not marked as such in the presentation of radar coverage by the manufacturer. If these areas are excluded from the computation, a probability of detection of 99.51 percent can be achieved.

4.3. User-Experience Test, Long-Term Evaluation

Evaluating the performance of the target detection scheme only during the above mentioned characteristic traffic situations is prone to error. The recorded radar data only shows the performance during a single instance of important traffic situations on the ground of the airport. Because of the workload of creating such evaluation sequences (which includes manual labeling of ground truth data), these sequences are also rather short with about 20 images per sequence and therefore the performance of the detection scheme can not be measured solely from the outcome of looking at these sequences. As there is only one recording for the distinct characteristic traffic situation, the performance could also only be evaluated for the weather conditions that were present during the time of recording.

To make sure that the target detection scheme performs well for all characteristic traffic within any weather condition, another evaluation methodology was applied additionally.

This evaluation methodology was a long-term analysis of the performance of the target detection scheme. This long term analysis was done at the reference site at Bucharest Otopeni Airport for comparability of the results.

The methodology for target detection presented in this thesis was deployed within the existing AviBit framework and was tested in a robustness phase lasting for two weeks.

During these two weeks, the air traffic controllers had a Human Machine Interface (HMI) (which visualizes the surveillance system outputs) set up at their workplace in the tower on site. The ATCOs were encouraged to report any kind of misbehavior or poor performance right away. For the sake of analysis and reproducability of possibly reported problems, the radar video was constantly recorded during the robustness phase. As the ATCOs are the end-users of the system, this test also functioned as a user-experience test. Not only does this evaluation test the performance of the detection scheme, but also its acceptance by the end-users who have extensive experience with using this type of system.

The only malfunction reports received during the robustness phase were reports of false targets at the sidelines of the runways. After analyzing the recordings, it was concluded that these false targets were produced by the metallic casing of runway guidance lights. These lights had previously not produced a radar echo strong enough to be detected as targets (their candidates were classified as non-target at the spatial classification step). During the time of the robustness test, there was a lot of rain and also some snow at Otopeni Airport and the wet metallic cases produced a much stronger echo in this case. As the lights are within the movement areas, no suppression of static targets was configured, which caused them to show up as targets on the HMI.

Overall, the end-users were satisfied with the performance of the system. The final acceptance for the ground surveillance system provided by AviBit was signed in early March 2014. The detection scheme presented in this work is a viable part of this system. The delivered ground surveillance system at Otopeni Airport is due to go operational in early 2015.

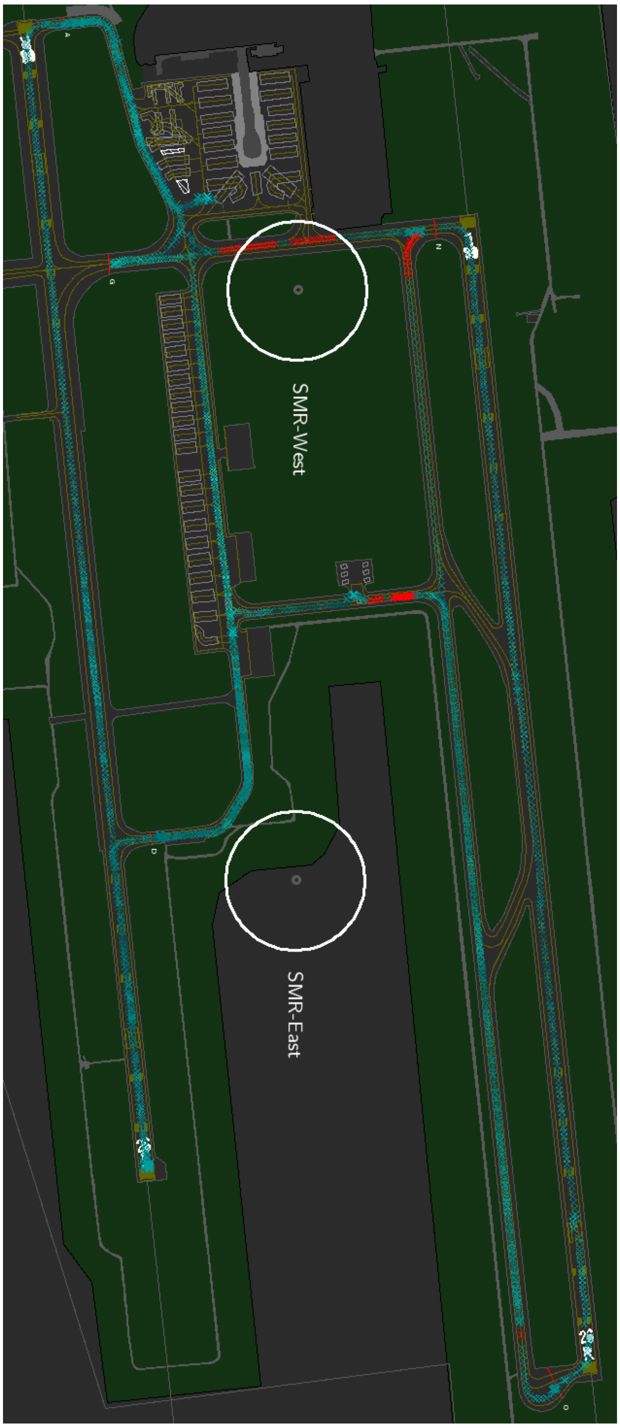

Figure 4.5.: Visualization of probability of detection analysis results (Both Radars, Tracked). Blue crosses are target detections, red crosses are missed target detection. Deadcones of radars visualized as white circles

5. Conclusion and Future Work

In this work, the problem of automated detection of security-relevant targets from SMR radar data in an airport ground surveillance context was tackled. A target detection scheme was presented, which in a first step pre-processes radar data using *CFAR* methods, which are common adaptive filtering methods in general radar signal processing. The scheme then forms target candidates based on properties elicited in a data analysis and classifies them into *target* and *non-target* returns according to available spatial and temporal information. To generate temporal information about objects in the surveillance area, they are tracked using *Interacting Multiple Model Kalman Filter Banks* using similarity measures for track association of the non-cooperative objects.

The presented target detection scheme was then evaluated based on available data sets from a reference setup at Bucharest Otopeni Airport. The evaluation included performance analysis for critical situations such as starts and landings of aircraft of different types and a *probability of detection* analysis for a target with known route. Moreover, a user experience or long-term evaluation was performed. For this purpose, air traffic controllers at Bucharest Otopeni Airport evaluated the performance of the target detection scheme in operational conditions over a duration of two weeks.

The results of the *probability of detection* analysis were satisfactory and showed that tracking and extrapolation of missed detections contingent on position predictions improve detection results. However, the results also showed that lack of physical coverage by the radars can only be improved in case of short losses of coverage and that the results are therefore still dependent on the quality of the radar setup (joint physical coverage of all areas of interest).

Results for the evaluation of starts and landings showed that despite taken measures in the target detection scheme, a number of false targets within Movement areas were reported. The reported false targets were induced either by radar reflections or other phenomena specific to the nature of operation of radar sensors. This observation is also aligned with the report of air traffic controllers after the long-term evaluation in an operational setting (who, however, were satisfied with the performance of the scheme otherwise). To overcome this issue for this work, the possibility was added to dynamically specify areas in which no tracks should be initiated. The idea is that air traffic controllers should manually ”mask” false targets as soon as the circumstance arises and monitor this situation regularly to remove the masking areas again once the false target disappears.

This means that the scheme cannot operate in a fully automated manner, but rather needs some manual intervention based on these shortcomings induced by the nature of the sensor. For future work, it should be investigated if the situation can somehow be overcome in an automated manner. For instance, in multi-radar setups, it could be tested to only initiate tracks if more than one radar reports a target at a position. This could overcome problems like reflection-induced false targets of a single sensor. In single radar setups or cases of singular coverage, this method would not work, however. Also, in case of echoes induced by water or snow this approach would also not work. An approach where some sort of background subtraction for static targets is performed might also be interesting to investigate. Such an approach would probably also require a manual verification, though.

The radars in use at Bucharest Otopeni Airport are digital radars of the newest generation, which already incorporate some means to reduce noise internally and provide generally good signal-to-noise ratios. These radars are therefore influenced less by dynamic clutter resulting from rain- or snowfall than older radars without hardware level clutter suppression. Especially analog radars are heavily influenced by those weather phenomena. It is desirable that the performance of the scheme is tested for data produced by an analog radar to verify that the performance achieved is similar to the results of digital radars of the newest generation.

In order to further improve the detection results, the possibility to move the processing to highly parallelized hardware such as GPU should also be investigated. This might make more complex processing possible, while ensuring that the real-time requirements of the application are still met.

Appendix

Abbreviations

A-SMGCS	Advanced Surface Movement Guidance and Control System
ATC	Air Traffic Control
ATCO	Air Traffic Control Operator
HMI	Human-Machine Interface
SMR	Surface Movement Radar
SNR	Signal-to-Noise Ratio
SCR	Signal-to-Clutter Ratio
CFAR	Constant False Alarm Rate
ADS-B	Automatic Dependent Surveillance-Broadcast
MSER	Maximally Stable Extremal Regions
PD	Probability-of-Detection

Appendix A.

Surface Movement Radars (SMR) for Airport Ground Control

SMRs are rotating radars, which like any radar, measure the distance from the radar to an object by sending out bursts of radio waves and measuring the time until the echo of the radio wave is received.

The strength or amplitude of the echo (the amount of energy measured in the receiver) depends on the grade of reflectivity, size and orientation of the object the radio wave first interferes with. Metal surfaces, like aircraft bodies or any other kind of vehicle on airport ground, will generally have good reflectivity properties and therefore yield strong echoes for radio waves sent out by the SMR.

A.1. Image Acquisition and Functionality

The output of one full rotation of an SMR is a circular 360-degree image of radar echoes of the radar's surroundings. The radius of the circle is dependent on the range of the radar in use (typically used radars achieve a maximal radial range of about three kilometers). The radar's angle of rotation is called azimuth. Figure A.1 shows a sample installation of an SMR at Tallinn airport.

Figure A.1.: A sample SMR installation at Tallinn airport.

The resolution of an SMR image depends on the number of discrete azimuth steps that the SMR splits a full rotation into. One such step with fixed azimuth is called a “radar beam“ (see the green line in Figure A.4). Typically, SMRs split a full rotation into 4096 to 8192 radar beams (azimuth steps). This number of beams is dependent on the ”trigger” time of the radar (the time span between sending out beams while rotating). Secondly, the SMR image resolution is dependent on the number of radar echoes or radar samples along such a beam. That is, the number of radio waves sent out across the range of a radar beam with varying vertical angles (see Figure A.3). This results in radar samples in an interval of one to several meters up to the maximal radial range, depending on the radar in use. Because of the discrete azimuth steps, two consecutive radar beams diverge in radial distance of the radar. Consequently, the area a radar sample covers depends on the radial distance from the SMR. The degree of detail decreases along radial distance as the area a radar sample covers grows (this is depicted in Figure A.2). The *dead-cone* of a SMR is a circular area around the radar center in which no detection is possible. This is also visualized in Figure A.2 as the empty circle around the center.

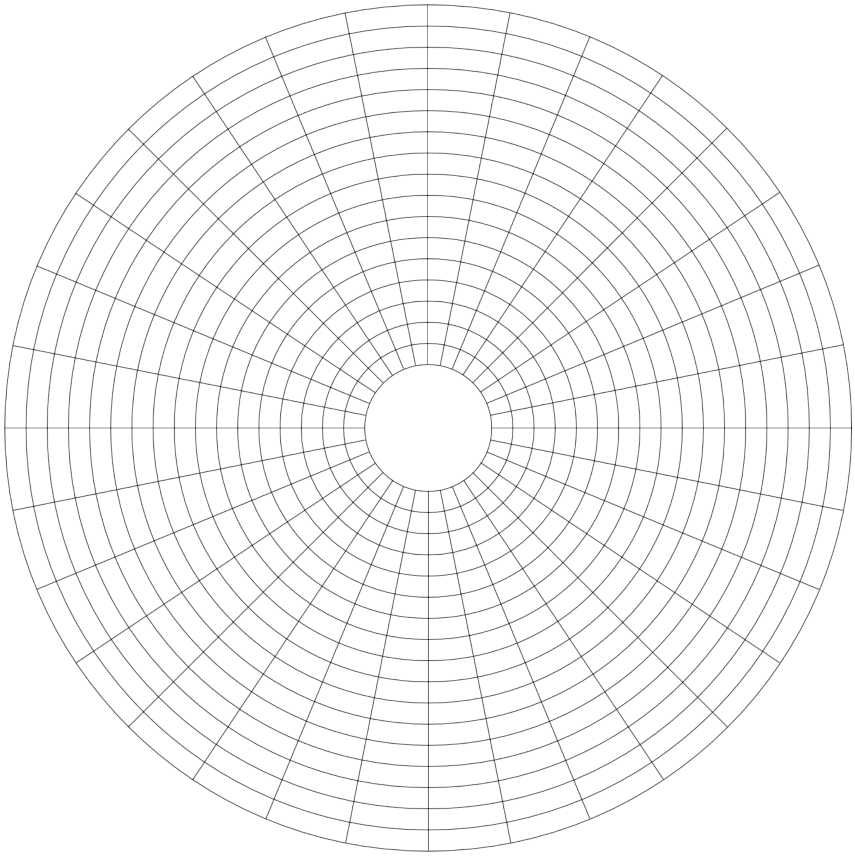

Figure A.2.: Visualization of tangentially growing samples with radial distance of the radar sensor

The received radar echoes for every sample are digitized. Typically, analog radar echoes are logarithmically converted into 8-bit values, representing the amplitude of the echo in logarithmic scale. This results in a range of 0 - 255 as possible values for representing the amplitude of the radar echo.

Figure A.3 shows what is commonly known as the *Radar Shadowing* effect. The nature of the radar sensor causes objects which are obstructed by other larger objects to be invisible to the radar. As the sample installation in Figure A.1 shows, the radars are installed in elevated locations to cover more grounds and reduce radar shadowing effects.

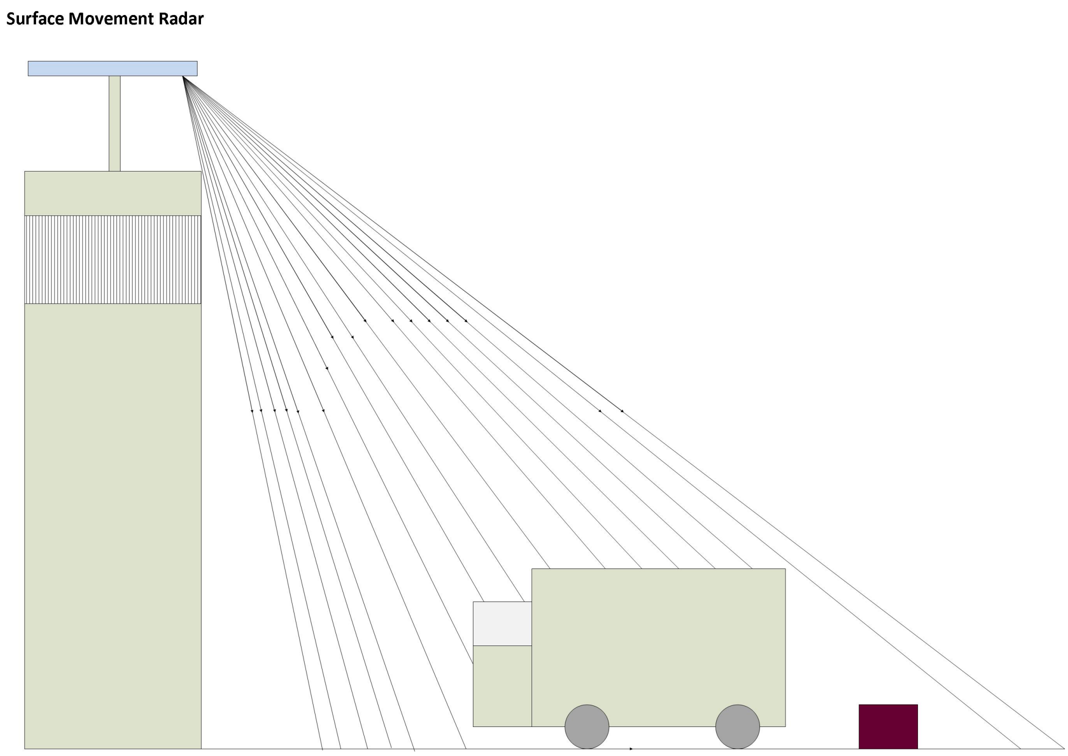

Figure A.3.: The radar shadowing effect (red object is obstructed by the truck)

A.2. Clutter and Noise in SMR Images

Figure A.4 shows a sample cutout of a raw SMR image of Hamburg Airport recorded during good weather conditions. This sample shows that aircrafts and vehicles on the apron result in strong radar echoes, as do the buildings and cement edges in the right part of the image.

Strong rain- and snowfall result in a rise of the overall signal levels and actual targets (such as aircrafts, vehicles or other objects in airport movement areas) are made less distinguishable from the noise. In other words, the *signal-to-noise ratio* (SNR) is smaller than in a less noisy case with better weather conditions (Figure A.4).

In radar signal processing, usually such unwanted high echo levels are called clutter rather than noise (to distinguish it from noise associated with the acquisition process), therefore the previously mentioned SNR would be called *signal-to-clutter ratio* (SCR).

Buildings, cement edges or metallic objects in non-movement areas are called static clutter, as they are unwanted high signal levels and do not move.

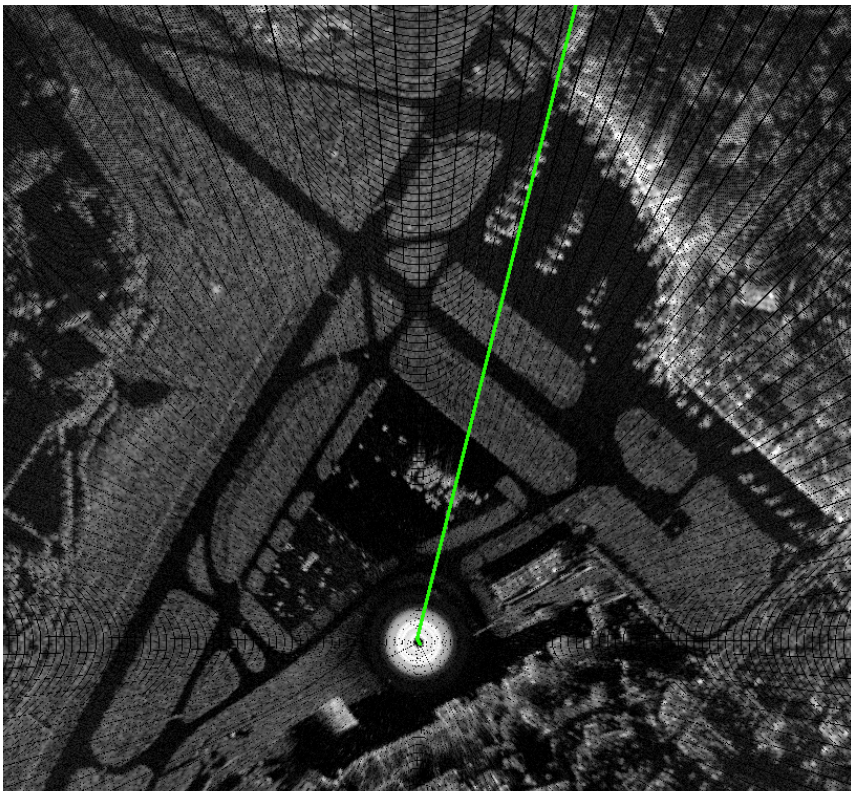

Figure A.4.: Sample SMR image of Hamburg Airport recorded during good weather conditions (cutout)

Figure A.5 shows a raw SMR image of the same area recorded during a heavy rain shower. Compared to Figure A.4, this image appears a lot more cluttered, especially on the runway in the left upper section of the image. This is due to the nature of the image acquisition process, as the falling raindrops are highly reflective and result in strong echoes of the radio waves at the receiver of the SMR. Snowflakes also have the property of high reflectivity of radio waves and therefore cause the same high clutter levels. A similar effect on a smaller scale can also be observed with long, wet grass on fields adjacent to airport movement areas. These effects are called dynamic clutter, as they vary in time, position and spatial expansion.

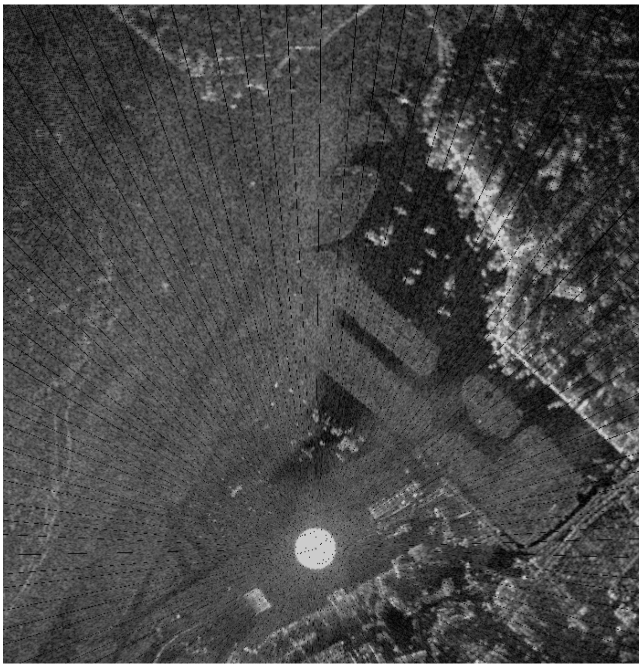

Figure A.5.: Sample SMR image of Hamburg airport recorded during bad weather conditions (cutout)

Figure A.5 also shows that rain showers (and hence dynamic clutter) can be very local and do not necessarily spread over the whole airport area. The right upper section of the image is less cluttered compared to the rest of the image. During the time this image was recorded a heavy local rain shower went down over the runways, but was less severe over the parking positions and gates in the right upper section of the image.

Appendix B.

Reference Radar Setup at Bucharest Airport

This section gives an overview of the reference setup at Bucharest Otopeni Airport, from which all data used in this thesis was collected.

At the reference site, two identical radars are installed to jointly cover all of the movement areas on the airport premises. The positioning of the radar on a schematical airport map is shown in Figure B.1 below. The radars have a trigger time of 0.244 milliseconds, which results in 4096 discrete azimuth steps or *beams* for a full rotation of the radar (corresponds to an angle of 0.0878 degrees between two radar beams). The radar has a radial resolution of three meters per radar range cell and a "dead cone" of about 200 meters in radial distance of the radar (within the dead cone of an SMR no radar echoes are received). As described in Section A.1 and visualized in Figure A.2, radar cells grow in radial distance from the radar. The size of radar cells for the radars in use is schematically shown in Table B.1.

The reflected energy of each radar sample is digitized into 8-bit values, according to the ratio of sent and received energy. An overview map of the site and the location of the installed SMRs is depicted in Figure B.1 below (not to scale). Figures B.2 and B.3 show areas on the airport without physical coverage for both radars due to occlusion by buildings on site.

Distance	Radar Sample Resolution
300 m	3 m radial x 0.5 m azimuth
500 m	3 m radial x 0.75 m azimuth
1000 m	3 m radial x 1.5 m azimuth
2000 m	3 m radial x 3 m azimuth
3000 m	3 m radial x 4.5 m azimuth

Table B.1.: Radar sample sizes in radial distance of the radar for reference setup at Bucharest Airport

Figure B.1.: Map of the Bucharest Otopeni Airport with the locations of the SMRs installed on site marked in white

Figure B.2.: Visualization of areas without radar coverage due to "shadowing" for SMR-West at Bucharest Airport (in red)

Figure B.3.: Visualization of areas without radar coverage due to "shadowing" for SMR-East at Bucharest Airport (in dark blue)

Bibliography

[1] Blom H. A. P., Bar-Shalom Y. The interacting multiple model algorithm for systems with Markovian switching coefficients. *Automatic Control, IEEE Transactions on*, 33(8):780–783, August 1988.

[2] Conte E., Lops M. Clutter-map CFAR detection for range-spread targets in non-Gaussian clutter. I. System design. *IEEE Transactions on Aerospace and Electronic Systems*, 33(2):432–443, 1997.

[3] Conte E., Lops M., Tulion A.M. Hybrid procedure for CFAR in non-Gaussian clutter. *IEE Proceedings in Radar, Sonar and Navigation*, 144(6):361–369, 1997.

[4] Di Vito A., Galati G. , Mura R. Analysis and comparison of two order statistics CFAR systems. *IEE Proceedings Radar, Sonar and Navigation* , 141(2):109–115, 1994.

[5] Ebrahimian Z. In *Proceedings of the International Conference on Wireless Communications and Applied Computational Electromagnetics (IEEE/ACES)*, pages 1045–1049, 2005.

[6] Farrouki A., Barkat M. Automatic censoring CFAR detector based on ordered data variability for nonhomogeneous environments. *Radar, Sonar and Navigation, IEE Proceedings*, 152, 2005.

[7] Ferri M., Galati G., Marti F., Naldi M. Advanced airport surveillance and imaging using the surface miniradar network. In *Proceedings of CIE International Conference of Radar*, Beijing, China, 1996.

[8] Ferri M., Galati G., Naldi M., Patrizi E. CFAR techniques for millimetre-wave miniradar. In *Proceedings of CIE International Conference of Radar*, Beijing, China, 1996.

[9] Finn H.M., Johnson R.S. *Adaptive detection mode with threshold control as a function of spatially sampled clutter estimation*, volume 29, pages 414–464. RCA Review, 1968.

[10] Gonzalez R., Woods R. *Digital Image Processing (3rd Edition)*. Prentice Hall, 3rd edition, 2007.

[11] Hansen V.G., Sawyer J.H . Detectability loss due to greatest of selection in a cell-averaging CFAR. *IEEE Transactions on Aerospace and Electronic Systems*, AES-16(1):115–118, 1980.

[12] He Y. Performance of some generalised modified order statistics CFAR detectors with automatic censoring technique in multiple target situations. *IEE Proceedings Radar, Sonar and Navigation* , 141(4):205–212, 1994.

[13] He Y. , Meng X. , Peng Y. Performance of a new CFAR detector based on trimmed mean. In *Proceedings of IEEE International Conference on Systems, Man and Cybernetics*, pages 702–706, Beijing, China, 1996.

[14] Khoury E.N., Hoyle J.S. Clutter maps: design and performance. In *Proceedings of National Radar Conference*, Atlanta, USA, 1984.

[15] Lops M., Orsini M. Scan-by-scan averaging CFAR. *IEE Proceedings of Radar and Signal Processing*, 136(6):249–254, 1989.

[16] Matas J., Chum O., Urban M., Pajdla T. Robust wide baseline stereo from maximally stable extremal regions. In *Proceedings of British Machine Vision Conference (BMVC)*, pages 384 – 396, 2002.

[17] Nitzberg R. Clutter Map CFAR Analysis. *IEEE Transactions on Aerospace and Electronic Systems*, 22(4):419–421, 1986.

[18] Palmieri F., Boncelet C.G Jr. Ll-Filters - A New Class of Order Statistic Filters. *IEEE Transactions on Acoustics, Speech and Signal Processing*, 37(5):691–701, 1989.

[19] Kalman R.E. A new approach to linear filtering and prediction problems. *Transactions of the ASME-Journal of Basic Engineering*, 82(Series D):35–45, 1960.

[20] Rohling H. Radar CFAR Thresholding in Clutter and Multiple Target Situations. *IEEE Transactions on Aerospace and Electronic Systems*, AES-19(4), 1983.

[21] Rohling H. 25 years Research in Range CFAR Techniques. In *Proceedings of the International Radar Symposium (IRS)*, Dresden, Germany, 2003.

[22] Rohling H. Ordered Statistic CFAR Technique - an Overview. In *Proceedings of the International Radar Symposium (IRS)*, Leipzig, Germany, 2011.

[23] Smith M.E, Varshney P.K. Intelligent CFAR processor based on data variability. *IEEE Transactions on Aerospace and Electronic Systems*, 36(3):837–847, 2000.

[24] Fox D. Thrun S., Burgard W. *Probabilistic Robotics (Intelligent Robotics and Autonomous Agents)*. The MIT Press, 2005.

[25] Weiss M. Analysis of some modified cell-averaging CFAR processors in multiple-target situations. In *IEEE Transactions on Aerospace and Electronic Systems*, number 18, pages 102–114, 1982.

[26] Xu C. , He Y. ,Yao Q. , Jian T. A modified robust CFAR detector. In *Proceedings of the Internation Conference on Electronic and Mechanical Engineering and Information Technology (EMEIT)*, pages 4439–4442, Harbin, Heilongjiang, China, 2011.

[27] Zhang R., Zou Y., Sheng W., Wang H. An Improved CFAR Detector for Nonhomogeneous Clutter Environment. In *Proceedings of International Symposium on Signals, Systems and Electronics (ISSSE2010)*, pages 1–4, Nanjing, China, 2010.

[28] Zhao J., Tao R., Wang Y. A New CFAR Detector Based on Ordered Data Variability. In *Proceedings of the First International Conference on Innovative Computing, Information and Control (ICICIC)*, pages 628–631, 2006.